Advanced multiconfiguration methods for complex atoms: Part I - Energies and wave functions

Charlotte Froese Fischer§

Atomic Spectroscopy Group, National Institute of Standards and Technology, Gaithersburg, MD 20899−8422, USA

Michel Godefroid

Chimie Quantique et Photophysique, CP160/09 Université libre de Bruxelles, B 1050 Bruxelles, Belgium

Tomas Brage

Division of Mathematical Physics, Department of Physics, Lund University, Box 118, SE-221 00 Lund, Sweden

Per Jönsson

School of Technology, Malmö University, S-20506, Malmö, Sweden

Gediminas Gaigalas

Institute of Theoretical Physics and Astronomy, Vilnius University, A. Goštauto 12, LT-01108, Vilnius Lithuania

Abstract. Multiconfiguration wave function expansions combined with configuration interaction methods are a method of choice for complex atoms where atomic state functions are expanded in a basis of configuration state functions. Combined with a variational method such as the multiconfiguration Hartree-Fock (MCHF) or multiconfiguration Dirac-Hartree-Fock (MCDHF), the associated set of radial functions can be optimized for the levels of interest. The present review updates the variational MCHF theory to include MCDHF, describes the multireference-single and double (MRSD) process for generating expansions and the systematic procedure of a computational scheme for monitoring convergence. The present review focuses on the calculations of energies and wave functions from which other atomic properties can be predicted such as transition rates, hyperfine structures and isotope shifts, for example.

PACS numbers: 31.15A-,31.15ag, 31.30J-, 32.70.Cs

Submitted to: *J. Phys. B: At. Mol. Phys.*

§ To whom correspondence should be addressed (Charlotte.Fischer@nist.gov)

Contents

Compiled on 2016/01/23 at 13:08:13

Compiled on 2016/01/23 at 13:08:13

1. Introduction

Atomic physics was the original testing ground for the new-born quantum theory close to a century ago, both regarding the non-relativistic theory by Schrödinger [1] and the relativistic theory by Dirac [2, 3]. Just a few years after this change of paradigm in physics, computational methods were introduced, to deal with models for systems other than the simplest hydrogen-like one [4, 5, 6]. Since then, the development of computational methods has been closely linked to dealing with new challenges in atomic physics - from atomic spectroscopy that was introduced and flourishing in the 1900's [7, 8], to the high-order, harmonic generation in ultra-high intense laser fields in recent days [9].

Today atomic physics is an important and very active branch of physics, both for its own sake while constantly finding new and exciting fields and applications, but also in support of other disciplines through data and fundamental insights. Atomic physicists are competing in high-profile journals and are active in many of the most prestigious laboratories in the world, including, e.g., CERN in the search for anti-Hydrogen [10].

To classify some of the most interesting fields of research and "Raison d'être" for atomic physics in general, and computational methods in particular, we can look at

(i) Many-body theory, since atomic systems represent the best known forces in physics.

(ii) Fundamental physics, since atomic experiments give unprecedented accuracy at a relatively low cost, opening up the possibility of performing extremely accurate measurements and finding small disturbances in exotic processes.

(iii) Plasma diagnostics in astrophysics, since most of the information about the Universe, consisting of ions and electrons, reaches us through electromagnetic radiation and most of the "visible" universe is in the plasma-state.

(iv) Complementing experiments, in a symbiotic relationship, in which the expensive and time consuming experiments are used to benchmark critically evaluated computational data, for diagnostics, and other purposes.

In this introduction we will start to describe this in more details, and then give an outline of this review.

1.1. Known forces

The forces or the potentials in atoms are well-known, in non-relativistic theory arguably exactly, and within the relativistic framework to very high precision. It is fair to say that the resulting theory of quantum electrodynamic (QED) is the best tested theory of interaction in physics where, e.g., its "coupling constant" - the fine structure constant - is known to 0.3 parts in a billion ($\alpha = 0.0072973525698(24)$) an unprecedented accuracy [11]. Since the forces are well understood, this opens up a unique possibility to study many-body effects - we know how to describe the nucleus-electron and electron-electron interactions. After starting with the independent particle model, we can therefore focus on what we will refer to as correlation - the complex dynamic behavior of electrons.

Compiled on 2016/01/23 at 13:08:13

1.2. Fundamental properties

It is clear that experimental atomic physics has reached accuracies that are unprecedented for determining, for example, relative energies of stationary states. If, at the same time, it is possible to develop accurate computational methods for the "known" atomic structure, it opens up the possibility of measuring small and minute effects, as a difference between the measured and computed results. If everything else is handled in a systematic fashion, these deviations could be interpreted as due to fundamental processes left out in the computational methods. This methodology has been applied to a wide range of fields, for example, the properties of exotic nuclei [12], violation of different fundamental symmetries [13], or the variation of the fine-structure constant with space and time [14, 15]. It is clear that atomic physics offers a unique and relatively speaking inexpensive way to investigate these topics.

1.3. Plasma diagnostics

The most important argument for investigation of atoms and ions is probably the fact that over 99% of all visible matter in the universe is in the plasma state [16] and many interesting features in the laboratory consist of plasmas. Since the constituents of a plasma are charged ions, together with electrons and photons, virtually all information we get on their properties is from the light they emit. This is the realm of atomic physics, where one predicts the light-emission of ions and how it is affected by the property of the plasma. If data for atomic transitions are known, the spectra from the plasma can give information about its fundamental properties, e.g., temperature and density (if they are well-defined), as well as the abundance of different elements and the balance between different ionization stages [17]. In some cases we are also able to determine magnetic fields - their strengths and polarization [18, 19].

In cases where the plasma is not in what is referred to as Local Thermal Equilibrium (LTE), even stronger demands are put on the atomic data, to be used in modeling [20, 21]. In addition, other atomic parameters such as line shapes, might be useful for different properties of the plasma. If we know the influence of the nucleus on the atomic structure, manifested by the so called hyperfine structure and isotope shifts, we can determine the isotopic composition of, e.g., astrophysical plasma - important to test different models of nucleosynthesis in the stars and in the interstellar medium [22, 23, 24, 25, 26, 27].

1.4. Complementing experiments

It is clear that experimental determination of the wealth of data needed is both extremely time consuming and expensive. Unfortunately, this has lead to a situation where very few experimental groups today are involved with atomic spectroscopy. At the same time, the need for data is increasing [28]. We mention three examples, where recent developments put great strain on atomic physics:

(i) Fusion power might be one of the energy sources for the future. To confine the fusion plasma, which has a temperature of millions of degrees, it is necessary to select the wall and divertor material with great care. The magnetic confinement is just not enough - there will always be some "stray" particles that will hit the wall of divertor. For the latter, it turns out that Tungsten could be the best choice [17]. It has excellent chemical properties, e.g., high heat conductivity

Compiled on 2016/01/23 at 13:08:13

and low melting point, but it also has a very complex atomic structure [29, 30]. When Tungsten atoms are sputtered and contaminate the plasma, the complex structure of the atom leads to the risk of heavy loss of energy due to many possible ways of radiating, and thereby also causing instabilities within the plasma. The complexity is also a hindrance to the necessary diagnostics of this contamination - very little is known about the structure of the different ions of Tungsten. A major effort in later years on the spectroscopy of Tungsten, has been to understand these complex systems and be able to help in developing a new energy source [31, 32, 33].

(ii) Recently some astrophysical missions and spectrographs (GIANO [34], CRIRES [35], SOFIA [36]) have moved into the infra-red wavelength region, making new objects visible and open for analysis. This is due to the fact that the infra-red light has a higher transmission through dust clouds, which are common in our galaxy and beyond. But, the long wavelength infra-red spectra are produced by transitions between levels lying close together in energy. Examples of this in atomic ions are transitions between highly excited states in, e.g., Rydberg series, and unexpected or forbidden transitions within ground configurations. Both of these are a challenge for experiment and need a strong support by accurate and systematic computations.

(iii) Also recently, a new form of experiments has been developed that has reached a realm of properties of observed matter and time scales considered impossible just a decade or two ago. It involves ion traps [37, 38] and storage rings [39, 40, 41] where very low densities - basically sometimes single ions - of highly charged plasma can be studied. This opens up the possibility to probe exotic processes in ions - such as forbidden and unexpected transitions from states with lifetimes of up to seconds or even hours [18]. Considering that "normal" lifetimes in ions are in the nanosecond range or less, the lifetimes of these long-lived states are to these "normal" lifetimes in ions as the age of the universe is to one single day. Modelling of the processes behind these transitions - whether it is nuclear spin-flips or high-order multipole interactions - is a true challenge to theory and probes our deep understanding of quantum mechanics.

The most efficient approach is therefore to use computations to model ions and benchmark these with selected and targeted experiments. With advances in technology, more and more properties are being predicted through computation, where comparison with experiment provides a validation and a mechanism for assessing the accuracy of a computational result.

1.5. Determination of accuracy

It is clear that data are needed, for different reasons. This requires a thorough understanding of the atomic system - consisting of a nucleus and a number of electrons, possibly is strong magnetic fields. In this review we will discuss one family of methods to deal with these systems. But it is not only important to find theoretical values of different properties - we also need to find a method to critically evaluate the data. There are basically two ways to approach this - either one derives theoretical expressions that give upper limits of the error in a computed result [42, 43], or one designs an approach that, in a systematic fashion, extends the complexity or simply the size of the calculations [44, 45, 46]. If the complexity could be described quantitatively, it is then possible to estimate the convergence of the calculations, or even extrapolate

Compiled on 2016/01/23 at 13:08:13

to give the deviation from the "exact" value [47, 48, 49, 50]. The methods we describe here offer a clear way to define a systematic approach since, as we will see in later sections, an atomic state is represented by an atomic state function, $\Psi(\Gamma J)$, which is expanded in a set of configuration state functions, $\Phi(\gamma_\alpha J)$,

$$\Psi(\Gamma J) = \sum_{\alpha=1}^{M} c_\alpha \Phi(\gamma_\alpha J). \tag{1}$$

The configuration state functions (CSFs) are created as linear combinations of products of members of an active set of orbitals, according to suitable angular momentum coupling rules for the case at hand. By extending the active set systematically, we increase the space spanned by the CSFs and thereby approach the complete space and the exact representation of the atomic state. As we will discuss later, this opens up a method for investigating the convergence of our method, which in turn will give an estimation of its accuracy.

1.6. A computational approach

In the present review, we focus on general *multiconfiguration* methods that determine a wave function for an atomic state in terms of a basis of configuration state functions as shown in Eq.(1). The basis states are constructed from one-electron orbitals (i.e. wave functions) that depend on the Hamiltonian under consideration. For light atoms, where the size of the nucleus is not a significant factor and relativistic effects can be adequately represented by first-order theory, the non-relativistic Hamiltonian may be used for determining orbitals. For heavier elements, where the effect of the nuclear size needs to be considered and a fully relativistic treatment is needed, the Dirac-Coulomb Hamiltonian is the basic Hamiltonian for one-electron orbitals. Various corrections may then be added including quantum electrodynamic (QED) effects.

The multiconfiguration Hartree-Fock (MCHF) method with Breit-Pauli corrections (MCHF+BP) and the multiconfiguration Dirac-Hartree-Fock (MCDHF) method with Breit and QED corrections (MCDHF+Breit+QED) represent these two approaches. Both are variational methods where the radial factors of orbitals are functions that optimize an energy expression. As a consequence, orbitals with a low generalized occupation are no longer "spectroscopic" and represent corrections to the wave function for the electron-electron cusp condition arising from the singularities in the Hamiltonian away from the nucleus [51]. The underlying variational formulation of these two theories differ in detail, but is very similar in concept. The same computational procedures can be used. In fact, many concepts are easier to explain in non-relativistic theory and we will do so here. Some of the variational theory for the MCHF method was presented in 1977 [52] , when MCHF expansions were small and before the systematic computational schemes developed in the early 1990s were introduced.

A significant advance in the last few decades has been the introduction of systematic methods that rely on single- and double (SD) excitations from a multi-reference set for generating wave function expansions. In a recent study, near spectroscopic accuracy was obtained for Si-like spectra consisting of nearly 100 levels with an expansion size of about a million [53]. The present review is restricted to the prediction of energies and wave functions – for all elements of the periodic table. It updates the variational MCHF theory to include MCDHF, describes the multireference single- and double- substitution (MRSD) process for generating expansions and the

Compiled on 2016/01/23 at 13:08:13

systematic procedure of a computational scheme for monitoring convergence. We refer to these as the MCHF-MRSD or MCDHF-MRSD computational procedures. The codes used for illustrative purposes are ATSP2K [54] and GRASP2K [55], respectively.

A more recent advance has been the introduction of B-spline methods in which integro-differential equations are replaced by generalized eigenvalue problems [56]. This facilitates the calculation of high-lying Rydberg states, but also provides a complete basis set of orbitals in a fixed potential, where the range is restricted to the range of an occupied orbital. As a consequence, they would have a "local" character. It is also possible to satisfy orthogonality conditions through the use of projection operators applied to the matrix eigenvalue problem. These methods will not be part of focus of this review.

2. The many-electron Hamiltonians

2.1. The non-relativistic Hamiltonian

In quantum mechanics, a stationary state of an N-electron atom is described by a wave function $\Psi(\mathbf{q}_1, .., \mathbf{q}_N)$, where $\mathbf{q}_i = (\mathbf{r}_i, \sigma_i)$ represents the space and spin coordinates, respectively, of the electron labeled i. The wave function is assumed to be continuous with respect to the space variables and is a solution to the wave equation

$$\mathcal{H}\Psi(\mathbf{q}_1, .., \mathbf{q}_N) = E\Psi(\mathbf{q}_1, .., \mathbf{q}_N), \tag{2}$$

where $\mathcal{H}$ is the Hamiltonian operator for the atomic system. For bound state solutions, the wave function must be square integrable and as a result of this, solutions exist only for discrete values of E that represent the total energy of the system.

The operator $\mathcal{H}$ depends on the quantum mechanical formalism and on the atomic system, including the model for the nucleus. For non-relativistic calculations, the starting point is the time-independent Schrödinger's equation (2) using the Hamiltonian for a nuclear point charge of infinite mass located at the origin of the coordinate system. In atomic units [11], this Hamiltonian is

$$\mathcal{H}_{NR} = \sum_{i=1}^{N} h(i) + \sum_{j>i=1}^{N} \frac{1}{r_{ij}} = \sum_{i=1}^{N} \left(-\frac{1}{2}\nabla_i^2 - \frac{Z}{r_i} \right) + \sum_{j>i=1}^{N} \frac{1}{r_{ij}}, \tag{3}$$

where $h(i)$ is the one-electron non-relativistic Schrödinger Hamiltonian of electron i moving in the Coulomb field of the nuclear charge Z, r_i is the electron-nucleus distance and r_{ij} is the distance between electron i and electron j. The one-electron terms on the right hand side describe the kinetic and potential energy of the electrons with respect to the nucleus, and the two-electron terms the Coulomb potential energy between the electrons. The latter terms introduce singularities into the wave equation, away from the origin, and are problematic in that they destroy the "separability" of the Hamiltonian $\mathcal{H}_{NR}$. It turns out, that even if we are not explicitly using what is called "Central-field approximation", it is useful to discuss the consequences of such a first approach. As we will see below, it will give us the form of the wave functions, which will be discussed in more detail in the next section. This approximation implies, that there is a central field such that

$$V_C(r_i) \approx -\frac{Z}{r_i} + \sum_{j>i=1}^{N} \frac{1}{r_{ij}}. \tag{4}$$

Compiled on 2016/01/23 at 13:08:13

The solutions, or eigenfunctions, of the Schrödinger equation can now be written in spherical coordinates as [57]:

$$\psi_{nlm_lm_s}(r,\theta,\varphi,\sigma) \;=\; \frac{P_{nl}(r)}{r}\; Y_{lm_l}\,(\theta,\varphi)\;\; \chi^{(1/2)}_{m_s}\,(\sigma)\,, \tag{5}$$

where l and $s = 1/2$ denote the orbital and spin quantum numbers, respectively, m_l and m_s specify the projections of $\mathbf{l}$ and $\mathbf{s}$ along the z-axis, and σ represents the spin variable. The principal quantum number n distinguishes solutions with the same set of other quantum numbers, but different energies. The condition $n > l$ assures that the power series expansion of the hydrogenic radial function terminates and the radial function is square integrable. The radial functions $P_{nl}(r)$ are solutions of the radial equation

$$\left(-\frac{1}{2}\frac{d^2}{dr^2} + V_C(r) + \frac{l(l+1)}{2r^2}\right) P_{nl}(r) = E\; P_{nl}(r)\;. \tag{6}$$

For the special hydrogen-like case where $N = 1$, the potential (4) reduces simply to $-Z/r$.

For bound states ($E < 0$), the radial equation only has solutions for eigenvalues $E \equiv E_n = -Z^2/(2n^2)\; E_\mathrm{h}$ (the Hartree unit for energy). With the eigenvalues being l-independent, the bound spectrum is highly degenerate ($g_n = 2n^2$). The radial functions $P_{nl}(r)$ are the well known hydrogen-like functions [57] with $n-l-1$ nodes. It is worthwhile to note that the functions (5) are also eigenfunctions of the parity operator Π where

$$\Pi\; \psi_{nlm_lm_s}(\mathbf{r},\sigma) = \psi_{nlm_lm_s}(-\mathbf{r},\sigma) = (-1)^l\; \psi_{nlm_lm_s}(\mathbf{r},\sigma)\;. \tag{7}$$

When $E = k^2/2 > 0$, the spectrum is continuous and the different solutions to the radial equation are labeled by k instead of n. In this case the radial function $P_{kl}(r)$ represents a free electron of momentum k [58, 59]. Though continuum processes are of great importance, this review will focus only on bound state solutions for atoms and ions.

2.2. The Dirac-Coulomb-Breit Hamiltonian

In the non-relativistic treatment it is formally straightforward to include the interaction between the electrons but, in the relativistic case, additional terms are needed since the instantaneous Coulomb interaction – electron-nucleus and electron-electron – is not Lorentz invariant and neglects the magnetic properties of the electron motion. Also, the speed of light (c) is finite in a relativistic model, and retardation effects need to be considered [60, 61]. A common approach is to combine the one-electron operators of the Dirac theory, with a nuclear potential, $V_{nuc}(r)$, corrected for an extended nuclear charge distribution function, instead of the one for a point charge. This yields the *Dirac-Coulomb* Hamiltonian, which in atomic units is [62]

$$\mathcal{H}_{DC} = \sum_{i=1}^{N} h_D(i) + \sum_{j>i=1}^{N} \frac{1}{r_{ij}} = \sum_{i=1}^{N} \left(c\;\boldsymbol{\alpha}_i\cdot\mathbf{p}_i + V_{nuc}(r_i) + c^2(\beta_i - 1)\right) + \sum_{j>i=1}^{N} \frac{1}{r_{ij}}, \tag{8}$$

where h_D is the one-electron Dirac operator (shifted for the energy to coincide with nonrelativistic conventions), $\boldsymbol{\alpha}$ and β are usual 4×4 Dirac matrices, c is the speed of light ($= 1/\alpha = 137.035999\ldots$ a.u.), and $\mathbf{p} \equiv -\mathrm{i}\boldsymbol{\nabla}$ the electron momentum operator. For the finite nucleus approximation, either a uniform nuclear charge distribution, or

Compiled on 2016/01/23 at 13:08:13

a more realistic nuclear charge density given by a Fermi distribution function is used. In both cases the root-mean square of the nuclear radius that enters in the definition of the nuclear potential changes from one isotope to another [63, 64].

If we use a central-field approximation

$$V_C(r_i) \;\approx\; V_{nuc}(r_i) \;+ \sum_{j>i=1}^{N} \frac{1}{r_{ij}} \;, \tag{9}$$

the problem becomes separable just as in the non-relativistic case, and the many-electron wave function can be expressed as a simple product of one-electron solutions of the Dirac equation with the central field, usually written as

$$\psi_{nlsjm}(r,\theta,\varphi) = \frac{1}{r}\begin{pmatrix} P_{nlj}(r)\;\Omega_{lsjm}(\theta,\varphi) \\ \mathrm{i}\;Q_{nlj}(r)\;\Omega_{\tilde{l}sjm}(\theta,\varphi) \end{pmatrix}, \tag{10}$$

where $P_{nlj}(r)$ and $Q_{nlj}(r)$ are the radial functions and $\Omega_{lsjm}(\theta,\varphi)$ are spherical two-spinors built from the coupling of the spherical harmonics $Y_{lm_l}(\theta,\varphi)$ and the spin functions $\chi^{(1/2)}_{m_s}$

$$\Omega_{lsjm}(\theta,\varphi) = \sum_{m_l m_s} \langle l m_l \tfrac{1}{2} m_s | jm\rangle \; Y_{lm_l}(\theta,\varphi)\; \chi^{(1/2)}_{m_s} \;, \tag{11}$$

with

$$\chi^{(1/2)}_{\frac{1}{2}} = \begin{pmatrix} 1 \\ 0 \end{pmatrix}, \qquad \chi^{(1/2)}_{-\frac{1}{2}} = \begin{pmatrix} 0 \\ 1 \end{pmatrix} \;. \tag{12}$$

Note that the spherical two-spinor for the large component ($P_{nlj}(r)$) depends on l whereas for the small component ($Q_{nlj}(r)$) it depends on a quantity denoted as $\tilde{l}$. The coupling in (11) requires $|l-1/2| \le j \le l+1/2$ and $m = -j, -j+1, .., j-1, j$. One can show that in the case of a field of spherical symmetry, the wave function is an eigenfunction of the parity operator introduced in (7). This in turn leads to the pair of two-spinors in (10) having opposite parity, which implies that $\tilde{l}$ and l are related to each other [65]

$$\tilde{l} = \begin{cases} l+1 & \text{for} \quad j = l+1/2 \\ l-1 & \text{for} \quad j = l-1/2 \;. \end{cases} \tag{13}$$

Introducing the quantum number κ as the eigenvalue of the operator $K = -1 - \boldsymbol{\sigma}\cdot\boldsymbol{l}$ through

$$\kappa = \begin{cases} -(l+1) & \text{for} \quad j = l+1/2 \quad (\kappa \text{ negative}) \\ +l & \text{for} \quad j = l-1/2 \quad (\kappa \text{ positive}) \end{cases} \;, \tag{14}$$

allows us to rewrite the eigenfunctions (10) simply as

$$\psi_{n\kappa m}(r,\theta,\varphi) = \frac{1}{r}\begin{pmatrix} P_{n\kappa}(r)\;\Omega_{\kappa m}(\theta,\varphi) \\ \mathrm{i}\;Q_{n\kappa}(r)\;\Omega_{-\kappa m}(\theta,\varphi) \end{pmatrix}. \tag{15}$$

The relationship between the spectroscopic notation and the angular momentum quantum numbers l, $\tilde{l}$, j and κ is shown in table 1. It should be noted that each state is uniquely specified by κ.

Since the spin-angular functions are linearly independent, we can separate out the radial parts of the one-electron functions to get

$$\begin{aligned} &(V_C(r) - E\;)\;P_{n\kappa}(r) - c\left(\frac{d}{dr} - \frac{\kappa}{r}\right) Q_{n\kappa}(r) \qquad\quad = 0 \;, \\ &c\left(\frac{d}{dr} + \frac{\kappa}{r}\right) P_{n\kappa}(r) + \left(V_C(r) - 2c^2 - E\;\right)\;Q_{n\kappa}(r) = 0 \;, \end{aligned} \tag{16}$$

Compiled on 2016/01/23 at 13:08:13

Table 1. Spectroscopic notation of relativistic shells.

	$s_{1/2}$ s	$p_{1/2}$ p_-	$p_{3/2}$ p_+	$d_{3/2}$ d_-	$d_{5/2}$ d_+	$f_{5/2}$ f_-	$f_{7/2}$ f_+	$g_{7/2}$ g_-	$g_{9/2}$ g_+
l	0	1	1	2	2	3	3	4	4
$\tilde{l}$	1	0	2	1	3	2	4	3	5
j	1/2	1/2	3/2	3/2	5/2	5/2	7/2	7/2	9/2
κ	-1	$+1$	-2	$+2$	-3	$+3$	-4	$+4$	-5

where the zero of the energy scale has been shifted to correspond to the electron detachment limit, as in non-relativistic theory. For the special case of $N = 1$ and $V_C(r) = -Z/r$, the bound state solutions where $-2(m)c^2 \leq E \leq 0$ are well known. The functions $(P_{n\kappa}(r), Q_{n\kappa}(r))$ and the corresponding eigenenergies $E \equiv E_{n\kappa}$ depend on the n and κ quantum numbers (see for instance [62, 66]). The number of nodes in the large component $P_{n\kappa}(r)$ is $n - l - 1$, as in the non-relativistic case. The number of nodes in $Q_{n\kappa}(r)$ is $n - l - 1$ for $\kappa < 0$ but $n - l$ for $\kappa > 0$ [64]. It is worthwhile to emphasize the fact that for a given n, the solutions for $\pm\kappa$ are degenerate (e.g. $2s_{1/2}$ and $2p_{1/2}$), which preserves the degeneracy in l as we observed for the non-relativistic case. This, of course, is not true for a general central potential, but a special property of the Coulomb potential.

For the relativistic description of the many-electron system, the Dirac-Coulomb Hamiltonian (8) is only the first approximation and is not complete. To represent the corrections from the so called transverse photon interaction, we can use an approximation of order α^2:

$$\mathcal{H}_{TP} = -\sum_{j>i=1}^{N} \left[\frac{\boldsymbol{\alpha}_i \cdot \boldsymbol{\alpha}_j \, \cos(\omega_{ij} r_{ij}/c)}{r_{ij}} + (\boldsymbol{\alpha}_i \cdot \boldsymbol{\nabla}_i)(\boldsymbol{\alpha}_j \cdot \boldsymbol{\nabla}_j) \frac{\cos(\omega_{ij} r_{ij}/c) - 1}{\omega_{ij}^2 r_{ij}/c^2} \right], \quad (17)$$

to represent the magnetic interactions and the retardation effects [64, 67]. In this expression the $\boldsymbol{\nabla}$-operators act only on r_{ij}, while ω_{ij} represents the energy of the virtual exchanged photon between two electrons introduced in *quantum electrodynamics* (QED), even in the absence of the emission or absorption of "real" radiation. In the second quantization form of the interaction, which will be discussed later, ω_{ij} can be interpreted in terms of differences in orbital one-electron energies.

In the low photon energy limit, when $\omega_{ij} \to 0$, the expression (17) reduces to the Breit interaction [68]

$$\mathcal{H}_{Breit} = -\sum_{j>i=1}^{N} \frac{1}{2r_{ij}} \left[(\boldsymbol{\alpha}_i \cdot \boldsymbol{\alpha}_j) + \frac{(\boldsymbol{\alpha}_i \cdot \mathbf{r}_{ij})\,(\boldsymbol{\alpha}_j \cdot \mathbf{r}_{ij})}{r_{ij}^2} \right]. \quad (18)$$

Adding (17) to the Dirac-Coulomb Hamiltonian (8) gives the Dirac-Coulomb-Breit Hamiltonian (in the effective Coulomb gauge)

$$\mathcal{H}_{DCB} = \mathcal{H}_{DC} + \mathcal{H}_{TP} \simeq \mathcal{H}_{DC} + \mathcal{H}_{Breit} \, . \quad (19)$$

Compiled on 2016/01/23 at 13:08:13

Corrections to the Dirac-Coulomb-Breit Hamiltonian can be deduced from QED. The most important correction is the self-energy, which arises from the interaction of the electron with its own radiation field. For hydrogenic systems the electron self-energy can be expressed as

$$\Delta E_{SE} = \left(\frac{\alpha}{\pi}\right) \frac{\alpha^2 Z^4}{n^3} F(nlj, Z\alpha), \tag{20}$$

where $F(nlj, Z\alpha)$ is a slowly varying function of $Z\alpha$. The latter function has been derived by Mohr and co-workers [69, 70, 71] There have been no generalizations of the self-energy calculations to arbitrary N-electron atomic systems. Instead the total self-energy correction is given as a sum of one-electron corrections weighted by the fractional occupation number of the one-electron orbital in the wave function. Each one-electron contribution is expressed in terms of the tabulated hydrogenic values either by relying on a screened nuclear charge or by a scaling factor obtained from the Welton picture [72]. The most recent developments include also a non-local QED operator, which can be incorporated in the Dirac-Coulomb-Breit eigenvalue problem [73, 74].

The other important QED correction is the vacuum polarization correction, which is related to the creation and annihilation of virtual electron-positron pairs in the field of the nucleus. The vacuum polarization can be described by a correction to the Coulomb potential. For a nuclear charge distribution $\rho(r)$ the correction to the nuclear potential, referred to as the Uehling potential [75], is given by

$$V_{\mathrm{Uehl}}(r) = -\frac{2\alpha^2}{3r} \int_0^\infty r' \rho(r') \left[K_0(2c|r - r'|) - K_0(2c|r + r'|)\right] dr' \tag{21}$$

where

$$K_0(x) = \int_1^\infty e^{-xt} \left(\frac{1}{t^3} + \frac{1}{2t^5}\right) \sqrt{t^2 - 1}\, dt. \tag{22}$$

Terms of higher order can also be evaluated as the expectation value of potentials. Numerical evaluation of the expectation values relies on analytical approximations of the K_0 function by Fullerton and Rinker [76]. The above QED terms are included in the GRASP2K package [77] to yield the final Hamiltonian

$$\mathcal{H}_{DCB+QED} = \mathcal{H}_{DCB} + \mathcal{H}_{SE} + \mathcal{H}_{VP}\ . \tag{23}$$

2.3. The Breit-Pauli Hamiltonian

Dirac theory is a two-component theory in that both the large, $P(r)$, and the small, $Q(r)$, radial components are needed for the one-electron wave function. In the non-relativistic limit ($c \to \infty$) known as the Pauli approximation [64], the small component can be estimated from the large one [62], as

$$Q(r) = \left(\frac{\alpha}{2}\right) \left(\frac{d}{dr} + \frac{\kappa}{r}\right) P(r)\{1 + \mathcal{O}(\alpha^2)\}\ , \tag{24}$$

and the wave function again depends on only one component. The traditional method, however, is to modify the Hamiltonian. In the Breit-Pauli approximation, relativistic effects are accounted for by modifying the non-relativistic Hamiltonian (3) to include additional terms of order α^2 as an approximation of the Dirac-Coulomb-Breit operator and using non-relativistic radial functions [78, 79]. This Breit-Pauli Hamiltonian is often expressed as a sum over operators $\{H_i,\ i = 0, \ldots, 5\}$ introduced by Bethe and

Compiled on 2016/01/23 at 13:08:13

Salpeter [67], but it is also informative to separate the components according to their effect on the atomic energy spectrum as suggested by Glass and Hibbert [80], namely

$$\mathcal{H}_{BP} = \mathcal{H}_{NR} + \mathcal{H}_{RS} + \mathcal{H}_{FS}, \tag{25}$$

where $\mathcal{H}_{NR}$ is the non-relativistic many-electron Hamiltonian. The *relativistic shift* operator, $\mathcal{H}_{RS}$, commutes with $\mathbf{L}$ and $\mathbf{S}$ and can be written as

$$\mathcal{H}_{RS} = \mathcal{H}_{MC} + \mathcal{H}_{D1} + \mathcal{H}_{D2} + \mathcal{H}_{OO} + \mathcal{H}_{SSC}\ . \tag{26}$$

The *mass correction* term, $\mathcal{H}_{MC}$, represents a correction to the kinetic energy:

$$\mathcal{H}_{MC} = -\frac{\alpha^2}{8}\sum_{i=1}^{N}\nabla_i^4. \tag{27}$$

The next two interactions describe the one- and two-body *Darwin terms* $\mathcal{H}_{D1}$ and $\mathcal{H}_{D2}$, which are relativistic corrections to the nucleus-electron and electron-electron interactions, respectively. They are given by:

$$\mathcal{H}_{D1} = -\frac{\alpha^2 Z}{8}\sum_{i=1}^{N}\nabla_i^2\left(\frac{1}{r_i}\right) \quad \text{and} \quad \mathcal{H}_{D2} = \frac{\alpha^2}{4}\sum_{j>i=1}^{N}\nabla_i^2\left(\frac{1}{r_{ij}}\right). \tag{28}$$

The term $\mathcal{H}_{SSC}$ represents the Fermi-contact-type electron interaction contributing to the spin-spin interaction [81] and is therefore called the *spin-spin-contact* contribution [79]. It has the form

$$\mathcal{H}_{SSC} = -\frac{8\pi\alpha^2}{3}\sum_{j>i=1}^{N}\left(\mathbf{s}_i\cdot\mathbf{s}_j\right)\delta\left(\mathbf{r}_i\cdot\mathbf{r}_j\right)\ . \tag{29}$$

Finally $\mathcal{H}_{OO}$ is the *orbit-orbit* term, which represents the magnetic interaction between the magnetic moments of electron orbits,

$$\mathcal{H}_{OO} = -\frac{\alpha^2}{2}\sum_{j>i=1}^{N}\left[\frac{\left(\mathbf{p}_i\cdot\mathbf{p}_j\right)}{r_{ij}} + \frac{\left(\mathbf{r}_{ij}\left(\mathbf{r}_{ij}\cdot\mathbf{p}_i\right)\mathbf{p}_j\right)}{r_{ij}^3}\right]. \tag{30}$$

The *fine-structure* Hamiltonian $\mathcal{H}_{FS}$ describes magnetic interactions between the spin and orbital angular momenta of the electrons, and does not commute with $\mathbf{L}$ and $\mathbf{S}$, but only with the total angular momentum $\mathbf{J} = \mathbf{L} + \mathbf{S}$. It consists of three terms,

$$\mathcal{H}_{FS} = \mathcal{H}_{SO} + \mathcal{H}_{SOO} + \mathcal{H}_{SS}, \tag{31}$$

that induce the term splitting (fine structure). The largest contribution is, in most cases, the *spin orbit* interaction $\mathcal{H}_{SO}$ representing the interaction of the spin and angular magnetic momenta of an electron in the field of the nucleus

$$\mathcal{H}_{SO} = \frac{\alpha^2 Z}{2}\sum_{i=1}^{N}\frac{1}{r_i^3}\mathbf{l}_i\cdot\mathbf{s}_i. \tag{32}$$

The *spin-other-orbit* $\mathcal{H}_{SOO}$ and *spin-spin* $\mathcal{H}_{SS}$ contributions are interactions between magnetic moments related to the spin and orbital motion of *different electrons*

$$\mathcal{H}_{SOO} = -\frac{\alpha^2}{2}\sum_{i\neq j}^{N}\frac{\mathbf{r}_{ij}\times\mathbf{p}_i}{r_{ij}^3}\left(\mathbf{s}_i + 2\mathbf{s}_j\right)\ , \tag{33}$$

$$\mathcal{H}_{SS} = \alpha^2\sum_{j>i=1}^{N}\frac{1}{r_{ij}^3}\left[\mathbf{s}_i\cdot\mathbf{s}_j - 3\frac{\left(\mathbf{s}_i\cdot\mathbf{r}_{ij}\right)\left(\mathbf{s}_j\cdot\mathbf{r}_{ij}\right)}{r_{ij}^2}\right]. \tag{34}$$

Compiled on 2016/01/23 at 13:08:13

These spin-dependent operators usually produce a good representation of the fine structure splitting of terms in light to medium-sized atoms and ions. The spin-orbit interaction is the dominant term and behaves like Z^4. The spin-other-orbit reduces the size of the calculated fine structure splitting and scales as Z^3. The spin-spin interaction obeys the same Z^3 scaling law but, is two or three orders of magnitude smaller for most atomic systems [82].

3. The Configuration State Function

When the electron-electron interactions can be approximated by a central field, as in equations (4) or (9), the equations for the many-electron system become separable and the solutions are simply products of the one-electron orbitals (5) or (10). At the same time, total energies are sums of the orbital energies. Each one-electron orbital, or spin-orbital, is defined by a set of four quantum numbers, nlm_lm_s in the non-relativistic case, and $nljm$ or $n\kappa m$ in the relativistic case. Since the orbital energies do not depend on the magnetic quantum numbers m_l, m_s or m, there are many degeneracies and any linear combination of products with the same total energy is also a solution. Not all solutions are physical since electrons are indistinguishable fermions (the absolute square of the wave function will be independent of a coordinate exchange of two particles) and the wave function should be antisymmetric under coordinate exchange of two particles. This forces us to represent the wave function of a many-electron atom in terms of Slater determinants that identically vanish if two spin-orbitals have the same values of the four quantum numbers. Thus for allowed atomic states no two spin-orbitals can have the same values of the four quantum numbers. This is the exclusion principle originally discovered by Pauli in 1925 [83] and leads to the shell structure of an atom.

For a many-electron system, the non-relativistic Hamiltonian commutes with both the total orbital and spin angular momentum operators $\mathbf{L}$ and $\mathbf{S}$, and therefore also $\mathbf{L}^2$, L_z and $\mathbf{S}^2$, S_z, so that the exact solution to the wave equation Ψ can be chosen as an eigensolution of these operators (see Ref [84], Eq. (1.10)) with quantum numbers LM_LSM_S. This approximation often yields results for low ionization stages and light ions that are in good agreement with observation. This has led to the so called *LS-approximation*, very important in atomic physics, not the least for historical reasons. However, for getting "spectroscopic accuracy", the L- and S-symmetry ultimately needs to be broken in order to take relativity into account, making the corresponding quantum numbers LS "good" but not "perfect" anymore. On the other hand, the Dirac-Coulomb-Breit Hamiltonian and the Breit-Pauli Hamiltonian commute with $\mathbf{J} = \mathbf{L} + \mathbf{S}$, and therefore with the $\mathbf{J}^2$ and J_z operators. The corresponding quantum numbers JM are perfect quantum numbers, useful for representing the eigensolutions in relativistic cases for which symmetry-breaking due to the hyperfine interaction or external fields can be neglected.

Because the quantum numbers are different for the non-relativistic and relativistic cases, it will be clearer at this point to distinguish between the two cases.

3.1. Nonrelativistic CSFs and their construction

In the non-relativistic framework the Hamiltonian commutes with total angular and total spin operators. As a result, any physical solution corresponds to a symmetry-adapted linear combination of Slater determinants that is also an eigenfunction of

Compiled on 2016/01/23 at 13:08:13

these operators. This requirement splits the solutions into a number of LS terms of given parity and each such solution defines a configuration state function (CSF) with total quantum numbers LSM_LM_S. The construction of these eigenstates using the relevant angular and spin operators is described in the next subsection. The associated nl quantum numbers define a subshell, its occupation number w representing the number of electrons with the given nl quantum numbers.

For an N-electron atom or ion, a general configuration consists of m groups of equivalent electrons, namely

$$(n_1l_1)^{w_1}(n_2l_2)^{w_2}...(n_ml_m)^{w_m}, \qquad N = \sum_{i=1}^{m} w_i. \tag{35}$$

where w_i is the occupation number of subshell i.

3.1.1. A single subshell In the case of a configuration with only a single subshell, $(nl)^w$, we introduce the antisymmetric *configuration state function* (CSF), $\Phi\left((nl)^w\alpha\nu LSM_LM_S\right)$, where the additional numbers α and ν uniquely specify the considered state when there is more than one term with the same LS value. The seniority number ν, which will be discussed below, is needed for $l \geq 2$ subshells while an additional number α is introduced for shells with orbital angular momenta $l \geq 3$, i.e. for electrons from the f-, g-, ... shells to get the one-to-one classification of the energy levels [85].

Such a CSF can be built by using a recursive method in which the CSF for a state with w electrons is defined as a sum of products of antisymmetric CSFs for states with $w-1$ electrons (the parent states) coupled to a single electron nl state [86]. This process can be expressed in terms of coefficients of fractional parentage (CFPs) $(l^{w-1}\overline{\alpha\nu}\overline{LS}|\}l^w\alpha\nu LS)$, the parent states $\Phi\left((nl)^{w-1}\overline{\alpha\nu}\overline{LSM}_L\overline{M}_S\right)$, and an nlm_lm_s state for a single electron, namely

$$\begin{aligned}\Phi\left((nl)^w\alpha\nu LSM_LM_S\right) &\equiv |(nl)^w\ \alpha\nu LSM_LM_S\rangle \\ &= \sum_{\overline{\alpha\nu}\overline{LS}} \left|\left((nl)^{w-1}\overline{\alpha\nu}\overline{LS}, nl\right)\ \alpha\nu LSM_LM_S\right\rangle (l^{w-1}\overline{\alpha\nu}\overline{LS}|\}l^w\alpha\nu LS),\end{aligned} \tag{36}$$

The recurrence continues until $w = 1$, which is a trivial case since a single electron has no antisymmetry requirement.

The orbital and spin couplings, $\overline{\mathbf{L}} + \boldsymbol{\ell} = \mathbf{L}$ and $\overline{\mathbf{S}} + \mathbf{1/2} = \mathbf{S}$, involved in (36) require the use of the vector-coupling expansion for $\mathbf{j}_1 + \mathbf{j}_2 = \mathbf{J}$, namely

$$|\gamma_1j_1\gamma_2j_2\ JM\rangle = \sum_{\substack{m_1,\,m_2 \\ m_1+m_2=M}} |\gamma_1j_1m_1\rangle\ |\gamma_2j_2m_2\rangle\ \langle j_1j_2m_1m_2|j_1j_2JM\rangle\ , \tag{37}$$

where the coefficients $\langle j_1j_2m_1m_2|j_1j_2JM\rangle$ are the well-known Clebsch-Gordan coefficients [87, 88]. The CFP's are defined to ensure that the wave function is antisymmetric and thereby satisfies the Pauli exclusion principle. It is clear that they play a fundamental role in the theory of many-electron atoms. The final CSF for a single subshell separates into a radial and a spin-angular factor, according to

$$\Phi\left((nl)^w\alpha\nu LSM_LM_S\right) \equiv \left[\Pi_{i=1}^{i=w}P_{nl}(r_i)/r_i\right]|l^w\ \alpha\nu LSM_LM_S\rangle\ . \tag{38}$$

Compiled on 2016/01/23 at 13:08:13

3.1.2. Seniority and quasispin Racah introduced the seniority quantum number in a formal way [86, 89, 90]. It can be thought of as a classification of terms, with ν equal to the number of electrons in the subshell when it first occurs, say w_0. The next time this LS-term can occur is for $w = w_0 + 2$. If in this case there are two terms with the same LS-symmetry, we choose the seniority $\nu = w_0$ for the one formed by the coupling of $\Phi\left((nl)^2\ {}^1S(M_L = 0)(M_S = 0)\right)$ to the previous occurrence, as in

$$\begin{aligned}\Phi\left((nl)^{w_0+2}\,\alpha(\nu = w_0)LSM_LM_S\right)\\ = \Phi\left((nl)^{w_0}\overline{\alpha}\,(\overline{\nu} = w_0)\,LSM_LM_S\right)\Phi\left((nl)^2\ {}^1S(M_L = 0)(M_S = 0)\right)\end{aligned} \quad (39)$$

The second term with the same LS-symmetry, will be defined by seniority $\nu = w_0 + 2$ and coupled to be orthogonal to the first.

However, this has a group-theoretical interpretation based on the theory of quasispin [91, 92, 93, 94]. Briefly, if we define the quasispin quantum number Q as:

$$Q \;=\; \frac{1}{2}\;(2l + 1 - \nu)\,, \quad (40)$$

then it is possible to show that the corresponding operator will have the transformation and commutation properties of the spin momentum. The quantum number representing its projection will be

$$M_Q \;=\; \frac{1}{2}\;(w - 2l - 1) \quad (41)$$

and it shows the range of the number of electrons in the shell for a given l, in which the term LS, characterized by the quantum number ν, exists.

In the single subshell CSF notation, accounting for the quasispin Q and its projection M_Q, the CSF can then be written as [95]:

$$|(nl)^w\ \alpha\nu LSM_LM_S\rangle \;\equiv\; |nl\ \alpha QLSM_QM_LM_S\rangle\,. \quad (42)$$

3.1.3. Several subshells To construct a specific CSF associated with the configuration introduced in Eq (35) for multiple subshells, one starts with the products of the antisymmetric eigenfunctions for the different groups of equivalent electrons, namely

$$\begin{aligned}(\mathcal{Q}_1|(n_1l_1)^{w_1}\alpha_1\nu_1L_1S_1M_{L_1}M_{S_1}\rangle(\mathcal{Q}_2|(n_2l_2)^{w_2}\alpha_2\nu_2L_2S_2M_{L_2}M_{S_2}\rangle\ldots\\ \times(\mathcal{Q}_m|(n_ml_m)^{w_m}\alpha_m\nu_mL_mS_mM_{L_m}M_{S_m}\rangle,\end{aligned} \quad (43)$$

where $\mathcal{Q}_1$ represents the w_1 co-ordinates $\{\mathbf{q}_1, ..., \mathbf{q}_{w_1}\}$, $\mathcal{Q}_2$ the w_2 co-ordinates $\{\mathbf{q}_{w_1+1}, ..., \mathbf{q}_{w_1+w_2}\}$, etc., up to the final set $\mathcal{Q}_m$ $\{\mathbf{q}_{N-w_m+1}, ..., \mathbf{q}_N\}$ of the last m^{th} shell. With the repeated use of the vector-coupling expansion (37), we can couple the product functions to the final total angular momenta LSM_LM_S according to some specified coupling scheme. In this review as well as in ATSP2K and GRASP2K, the coupling applies from left-to-right and downwards, as shown graphically in Figure 1 for LS coupling. The orbital and spin angular momenta of the first two subshells are coupled to yield a resultant state $L_{12}S_{12}$. Then successively, until all subshells have been coupled, the next subshell is coupled to a resultant to form a new state. Each subshell-coupling uses the angular momenta coupling expansion (37) twice, first in the orbital space ($\mathbf{L}_{12\ldots(k-1)} + \mathbf{L}_k = \mathbf{L}_{12\ldots k}$), and then in the spin space ($\mathbf{S}_{12\ldots(k-1)} + \mathbf{S}_k = \mathbf{S}_{12\ldots k}$).

This procedure leads to a function, denoted by $\Phi_\wp(\gamma LSM_LM_S)^u$, which is antisymmetric with respect to co-ordinate permutations within each subshell, but

Compiled on 2016/01/23 at 13:08:13

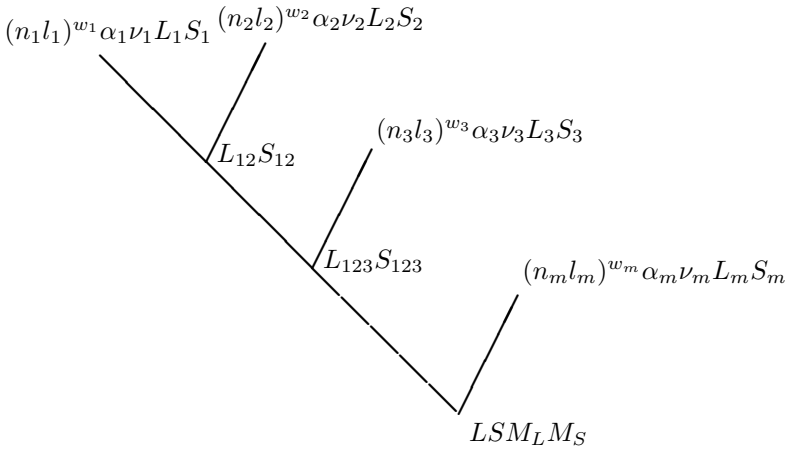

Figure 1. Coupling of subshells for a CSF in LS-coupling

not antisymmetric with respect to permutations between *different* subshells [96]. The additional antisymmetrization can, however, be accomplished through the restricted permutations

$$\Phi(\gamma LSM_LM_S) = \left(\frac{\prod_{a=1}^{m} w_a!}{N!}\right)^{1/2} \sum_{\wp} (-1)^p \Phi_{\wp}(\gamma LSM_LM_S)^u, \tag{44}$$

where the sum is over all permutations involving co-ordinate exchange only between two different subshells such that the co-ordinate number within each subshell remains in an increasing order. The antisymmetrizing permutations of electron coordinates between different subshells appreciably complicates the appearance of basis functions (44); however, these complications largely disappear in the evaluation of matrix elements of symmetric operators [87]. So, all this leads to the most general form of a CSF

$$\begin{aligned}
&\Phi(\gamma LSM_LM_S) \equiv |\gamma LSM_LM_S\rangle \\
&\equiv |(n_1l_1)^{w_1}\alpha_1\nu_1L_1S_1\ (n_2l_2)^{w_2}\alpha_2\nu_2L_2S_2\ L_{12}S_{12} \\
&\quad (n_3l_3)^{w_3}\alpha_3\nu_3L_3S_3\ L_{123}S_{123}...(n_ml_m)^{w_m}\alpha_m\nu_mL_mS_m\ LSM_LM_S\rangle\ ,
\end{aligned} \tag{45}$$

that in the quasispin representation (42), becomes

$$\begin{aligned}
&\Phi(\gamma LSM_LM_S) \equiv |\gamma LSM_LM_S\rangle \\
&\equiv |(n_1l_1)\alpha_1Q_1L_1S_1M_{Q_1}\ (n_2l_2)\alpha_2Q_2L_2S_2M_{Q_2}\ L_{12}S_{12} \\
&\quad (n_3l_3)\alpha_3Q_3L_3S_3M_{Q_3}\ L_{123}S_{123}...(n_ml_m)\alpha_mQ_mL_mS_mM_{Q_m}LSM_LM_S\rangle.
\end{aligned} \tag{46}$$

In this notation γ represents the configuration and all the intermediate quantum numbers that define the CSF. The configuration determines the parity $P = (-1)^{\sum_i^N l_i}$ of the CSF.

3.2. Relativistic CSFs

3.2.1. Single subshell CSF case In relativistic atomic theory, there are two possible $nlj = n\kappa$, orbitals for each nl nonrelativistic one when $l \neq 0$. Instead of the

Compiled on 2016/01/23 at 13:08:13

configuration state function $|(nl)^w\ \alpha\nu LSJ\rangle$, we then have to deal with a number of CSFs $|(nlj_1)^{w_1}\alpha_1\nu_1 J_1\ (nlj_2)^{w_2}\alpha_2\nu_2 J_2\ J\rangle$, with the restrictions that

$$0 \le w_1 \le 2j_1 + 1, \qquad 0 \le w_2 \le 2j_2 + 1, \qquad \text{and } w_1 + w_2 = w\ . \quad (47)$$

For subshells with angular momenta $j = \frac{1}{2}, \frac{3}{2}, \frac{5}{2}$, and $\frac{7}{2}$ corresponding to s^w, p^w, d^w, and f^w shells as well as $j = l - \frac{1}{2}$ of g^w shell, the seniority ν and J are sufficient to classify the relevant states. α becomes relevant when $j \ge 9/2$ to avoid any ambiguity.

A closed subshell is now defined by the quantum numbers nlj and, when $l \neq 0$, there will be two such subshells for each non-relativistic one. A closed subshell contains $2j + 1$ electrons. A separation of an electron configuration $(nl)^w$ into (jj-coupled) subshells is unique only for closed shells and for shells with a single vacancy. In general, several jj-coupled configurations with different distributions of the electrons can be found for each single non-relativistic configuration.

It is interesting to compare the different couplings for $3d^4$ ($J = 2$). For one non-relativistic *configuration* $3d^4$ spanning the eight ($J = 2$, even parity) CSFs, there are four relativistic configurations $3d_-^3 3d_+$, $3d_-^2 3d_+^2$, $3d_- 3d_+^3$ and $3d_+^4$.

Similar to the non-relativistic case, the quasispin quantum number Q of a relativistic subshell $|(nlj)^w\ \alpha\nu JM_J\rangle$ is simply related to the seniority quantum number ν by

$$Q = \left(\frac{2j+1}{2} - \nu\right)/2 \quad (48)$$

while M_Q, the eigenvalue of Q_z, depends on the occupation number w, namely

$$M_Q = \left(w - \frac{2j+1}{2}\right)/2. \quad (49)$$

The wave function of a subshell of w equivalent electrons and total angular momentum J can then be written in both the seniority and quasispin representations:

$$|(nlj)^w\ \alpha\nu JM_J\rangle\ \equiv\ |(n\kappa)^w\ \alpha\nu JM_J\rangle\ \equiv\ |n\kappa\ \alpha Q JM_Q M_J\rangle\ . \quad (50)$$

In analogy with (38), this function factorizes as a product of a radial factor (a 2×2 diagonal matrix containing the product of the large and small components, respectively) and a spin-angular vector

$$\begin{aligned}&\Phi\left((n\kappa)^w \alpha\nu JM_J\right)\\ &= \begin{pmatrix} \Pi_{i=1}^w P_{n\kappa}(r_i)/r_i & 0 \\ 0 & \Pi_{i=1}^w Q_{n\kappa}(r_i)/r_i \end{pmatrix} \left| \begin{pmatrix} (+\kappa)^w \alpha\nu JM_J \\ (-\kappa)^w \alpha\nu JM_J \end{pmatrix} \right\rangle\ . \end{aligned} \quad (51)$$

3.2.2. Multiple subshells The CSF for the vector-coupled shells are derived in a similar manner as in the non-relativistic case (see equations (45) and (46)), except that the J_i angular momenta are the only ones that need to be coupled. For instance, in the seniority representation, a general CSF takes the following form

$$\begin{aligned}&\Phi(\gamma JM_J) \equiv |\gamma JM_J\rangle\\ &\equiv |(n_1\kappa_1)^{w_1}\alpha_1\nu_1 J_1\ (n_2\kappa_2)^{w_2}\alpha_2\nu_2 J_2\ J_{12}\\ &\quad (n_3\kappa_3)^{w_3}\alpha_3\nu_3 J_3\ J_{123}...(n_m\kappa_m)^{w_m}\alpha_m\nu_m J_m\ JM_J\rangle\ , \end{aligned} \quad (52)$$

where γ represents the electron configuration in jj-coupling and all additional quantum numbers needed to completely specify the state.

Compiled on 2016/01/23 at 13:08:13

3.3. Variational methods for wave functions as a single CSF

Given a set or orthonormal radial functions, the set of CSFs with the same parity and LS or J quantum numbers defined by these radial functions form a basis for a function space of approximate wave functions, or atomic state functions (ASFs), denoted as Ψ. A very special case is the one where the wave function is expressed as a single CSF.

In our discussion so far, we have shown how the spin-angular factor of a CSF can be constructed assuming the radial functions were from a general central-field equation. The question then arises as to which radial functions yield the "best" approximate wave functions. Variational methods [97, 98] that optimize the total energy, result in equations for the radial functions known as Hartree-Fock (HF) equations in non-relativistic theory and Dirac-Hartree-Fock (DHF) in relativistic theory.

For a normalized wave function Ψ the total energy is the expectation value of the Hamiltonian (3), namely

$$E[\Psi] = \langle\Psi|\mathcal{H}|\Psi\rangle \quad \text{with the condition} \quad \langle\Psi|\Psi\rangle = 1. \tag{53}$$

When the definition of Ψ includes functions or constants that can be varied, the "best" wave function $\Psi^{\rm best}$ is the function for which the $\delta E = 0$ for all allowed perturbations $\delta\Psi$, orthogonal to Ψ and satisfying the boundary conditions, namely

$$\langle\delta\Psi|\mathcal{H} - E|\Psi^{\rm best}\rangle = 0\ . \tag{54}$$

When Ψ is assumed to be a single CSF, only the radial functions can be varied. Thus an expression for the energy in terms of radial functions is useful and is referred to as an *energy functional*. The orthogonality constraints must also be included in the variational process. As a result, the allowed perturbations, viewed as perturbations of the radial functions, are of two types – those that involve only a single radial function, and those that require that two radial functions be perturbed simultaneously in order to maintain orthonormality. Perturbations of more than two orbitals of the same symmetry can be expressed as a sequence of perturbations two at a time.

3.3.1. The Hartree-Fock equations Let $a, b, c, \ldots$ represent one-electron radial functions for an orthonormal set of spin-orbitals (5) with associated quantum numbers $n_a l_a, n_b l_b, n_c l_c, \ldots$. and $|\gamma LS\rangle$ the CSF for a configuration γ with LS quantum numbers. Since energies are independent of the M_L and M_S quantum numbers, these quantum numbers will be suppressed in the notation for the CSFs.

The HF equations are derived by applying the variational principle [52] to an expression for the total energy of the CSF based on the non-relativistic Hamiltonian (3). It can be shown that

$$\langle\gamma LS|\sum_{i=1}^{N} h(i)\ |\gamma LS\rangle = \sum_a w_a I(a,a), \tag{55}$$

where, in general,

$$I(a,b) = \delta(l_a,l_b)\langle P_a|-\frac{1}{2}\mathcal{L}\ |P_b\rangle \quad \text{and} \quad \mathcal{L} = \frac{d^2}{dr^2} + \frac{2Z}{r} - \frac{l(l+1)}{r^2}\ . \tag{56}$$

By using the expansion in terms of Legendre polynomials,

$$\frac{1}{r_{12}} = \sum_k \frac{r_<^k}{r_>^{k+1}} P_k(\cos\theta), \tag{57}$$

Compiled on 2016/01/23 at 13:08:13

where $r_< = \min(r_1, r_2)$ and $r_> = \max(r_1, r_2)$, the contribution from the two-electron operator becomes

$$\langle \gamma LS| \sum_{j>i=1}^{N} \frac{1}{r_{ij}} |\gamma LS\rangle = \sum_{abk} \left[f_{abk} F^k(ab) + g_{abk} G^k(ab) \right] , \tag{58}$$

where the sum is over pairs of orbitals, possibly from the same subshell. Here $F^k(ab) = R^k(ab, ab)$ and $G^k(ab) = R^k(ab, ba)$ are special cases of the more general Slater integral

$$R^k(ab, cd) = \langle P_a(r_1) P_b(r_2) | \frac{r_<^k}{r_>^{k+1}} | P_c(r_1) P_d(r_2) \rangle . \tag{59}$$

This integral is symmetric with regard to co-ordinate exchange as well as left/right exchange. The $F^k(ab)$ integrals are referred to as "direct" integrals in that the same orbitals are selected for the left/right pair whereas $G^k(ab)$ integrals are exchange integrals because they arise from the anti-symmetrizing exchange operator. Though defined as a double integral, Hartree [99] showed they could be evaluated efficiently through a pair of one-dimensional integrals:

$$Y^k(ab; r) = r \int_0^\infty \frac{r_<^k}{r_>^{k+1}} P_a(s) P_b(s) ds , \tag{60}$$

where $r_<$ ($r_>$) denotes the smaller (larger) of r and s so that

$$R^k(ab, cd) = \int_0^\infty P_a(r) P_c(r) \, \frac{1}{r} \, Y^k(bd; r) dr . \tag{61}$$

The spin-angular coefficients $\{w_a\}$, $\{f_{abk}\}, \{g_{abk}\}$ can be determined using the Slater-Condon rules for the Slater determinant algebra [100], or the Fano approach in the Racah-Wigner algebra [96]. In the last decade, a more efficient and general approach has been developed by Gaigalas *et al.* [101], combining second quantization in the coupled tensorial form, angular momentum theory in the orbital, spin and quasispin spaces, and graphical techniques. The relative simplicity of the energy expression (56) and (58) results from the orthonormality assumption for spin-orbitals (5)

$$\int \psi_a^*(\mathbf{r}, \sigma) \psi_b(\mathbf{r}, \sigma) \, d\mathbf{r} \, d\sigma = \delta_{ab} . \tag{62}$$

Due to the orthonormality property of the spherical harmonics and spin functions, this reduces to the radial orthonormality condition within each l-subspace,

$$\mathcal{C}_{ab} \equiv \langle P_a | P_b \rangle - \delta_{n_a n_b} = 0 . \tag{63}$$

The energy expression, along with Lagrange multipliers λ for orthonormality constraints (63) define the HF energy functional,

$$\begin{aligned} \mathcal{F}(\{P\}; \gamma LS) = & \sum_a w_a I(a, a) + \sum_{abk} \left[f_{abk} F^k(ab) + g_{abk} G^k(ab) \right] \\ & + \sum_{ab} \delta(l_a, l_b) \lambda_{ab} \mathcal{C}_{ab} . \end{aligned} \tag{64}$$

The first type of perturbation for which the functional must be stationary is $P_a \to P_a + \delta P_a$, where δP_a satisfies all boundary conditions and is orthogonal to all the occupied orbitals with the same symmetry. The perturbation for each term in the

Compiled on 2016/01/23 at 13:08:13

energy expression, when summed (see [56, 102]), is a function of the form $2\delta P_a K(a;r)$ so that the stationary condition becomes

$$\delta\mathcal{F} = 2\int_0^\infty \delta P_a(r) K(a;r) dr = 0, \quad \forall \text{ allowed } \delta P_a(r)\ . \tag{65}$$

This condition can only be satisfied if

$$K(a;r) \equiv 0. \tag{66}$$

Applying the stationary condition for the variation of each orbital a, results in a system of m coupled equations where m is the number of subshells. For a CSF (like $1s^2 2s$) with only two orbitals a, b with $nl, n'l$ quantum numbers, subject to orthogonality the two equations have the form [56]

$$\begin{bmatrix} H^a & 0 \\ 0 & H^b \end{bmatrix} \begin{bmatrix} P_a \\ P_b \end{bmatrix} - \begin{bmatrix} \varepsilon_{aa} & \varepsilon_{ab} \\ \varepsilon_{ba} & \varepsilon_{bb} \end{bmatrix} \begin{bmatrix} P_a \\ P_b \end{bmatrix} = 0, \tag{67}$$

where H^a, for example, is the integro-differential operator

$$H^a = w_a \left[-\frac{1}{2}\frac{d^2}{dr^2} - \frac{Z}{r} + \frac{l_a(l_a+1)}{2r^2} + Y(a;r) + \bar{X}(a;r) \right]. \tag{68}$$

Contributions to the direct potential $Y(a;r)$ arise from the $F^k(ab)$ integrals in the energy functional whereas contributions to the exchange potential $\bar{X}(a;r)$ arise from the $G^k(ab)$ terms. For the radial function $P_a(r)$, the latter integrals have the form $(Y^k(ab;r)/r)P_b(r)$. In other words, the function $P_a(r)$ is part of an integrand, making the equation an integro-differential equation of eigenvalue type when $\varepsilon_{ab} = 0$, in which case

$$w_a \bar{X}(a;r) P_a(r) = \sum_{bk} g_{abk} \left(\frac{Y^k(ab;r)}{r} \right) P_b(r). \tag{69}$$

In these equations, the matrix (ε_{ab}) is called the energy matrix [52] which in our definition is the same as the matrix of Lagrange multipliers. It has been customary to write differential equations so that the coefficient of the highest derivative is unity, which requires dividing each equation by $-w_a/2$. The latter has the consequence that the (ε_{ab}) matrix is no longer symmetric when the occupation numbers differ, even though $\lambda_{ab} = \lambda_{ba}$. When this convention is not followed and the epsilon matrix (ε_{ab}) is symmetric, it follows that

$$\begin{aligned} \varepsilon_{aa} &= \langle P_a | H^a | P_a \rangle, \quad \varepsilon_{ab} = \langle P_b | H^a | P_a \rangle, \\ \varepsilon_{ba} &= \langle P_a | H^b | P_b \rangle, \quad \varepsilon_{bb} = \langle P_b | H^b | P_b \rangle. \end{aligned} \tag{70}$$

The second type of perturbation relates to the "rotation" of orbitals in orbital space that in 2-dimensional space can be defined in terms of a single parameter $\epsilon \in [-1, 1]$ as in

$$\mathbf{O} = \begin{bmatrix} 1 & -\epsilon \\ \epsilon & 1 \end{bmatrix} / \sqrt{1+\epsilon^2}, \tag{71}$$

where $1/\sqrt{1+\epsilon^2} = \cos(\theta)$ and θ represents the angle of rotation. The radial transformation

$$\begin{bmatrix} P'_a(r) \\ P'_b(r) \end{bmatrix} = \begin{bmatrix} 1 & -\epsilon \\ \epsilon & 1 \end{bmatrix} \begin{bmatrix} P_a(r) \\ P_b(r) \end{bmatrix} / \sqrt{1+\epsilon^2}, \tag{72}$$

allows the effect of a rotation on the energy to be expanded in powers of ϵ, namely

$$E(\epsilon) = E(0) + g\epsilon + g'\epsilon^2 + \text{higher-order terms},$$

Compiled on 2016/01/23 at 13:08:13

where g represents the gradient of the energy with respect to rotation and $E(0)$ is the energy before orbitals are rotated. Then the stationary condition

$$\partial E/\partial\epsilon = 0 = g + 2g'\epsilon, \tag{73}$$

leads to $\epsilon = -g/(2g')$. When this condition is satisfied, $\varepsilon_{ab} = \varepsilon_{ba}$. Rules for determining g and g' from the energy expression are given in Ref. [102].

In the simple case of the HF equation for $1s2s\ ^1S$ where

$$E = I(1s,1s) + I(2s,2s) + F^0(1s2s) + G^0(1s2s)$$

the condition for a stationary solution is

$$R^0(1s1s;1s2s) - R^0(2s2s;2s1s) = 0. \tag{74}$$

Eq. (73) not only determines g (the amount by which the stationary condition is not satisfied) but also how much the radial functions used for evaluating the expression, need to be rotated for a stationary solution. When more that two radial functions are connected through orthogonality, variationally the energy should be stationary for *all* rotations, a condition that will be satisfied if it is stationary for the rotation of *all pairs* of radial functions and any unitary transformation.

Several properties of the HF solutions follow from these considerations.

3.4. Koopmans' theorem

The diagonal energy parameter $\varepsilon_{nl,nl} \equiv \varepsilon_{aa}$ (see (70)) for a singly occupied shell can easily be shown to be directly related to the binding energy of the nl electron, namely the difference in energy on the N-electron system and the energy of the $N-1$ electron system in which the nl electron has been removed, using the same set of radial functions for both the N and $N-1$ electron system [52, 84]. In general,

$$\varepsilon_{nl,nl} = E^{\rm HF}(\gamma LS) - \bar{E}((nl)^w) + \langle (nl)^w | \sum_{j<i} \frac{1}{r_{ij}} | (nl)^w \rangle \ , \tag{75}$$

where $\bar{E}((nl)^w)$ is the energy of the atomic system when the $(nl)^w$ subshell has been removed and the remaining term is a correction relating to the self-interaction within the subshell when is multiply occupied with $w > 1$. This is the usual Koopmans' theorem [103, 104] that has been used successfully for estimating many ionization energies.

The HF equations may not always have unique solutions. Consider the case of $1s^22s^2$ where the CSF can be expressed as a single Slater determinant. A unitary transformation (or rotation of the orbitals) changes the radial functions, but leaves the wave function and the total energy invariant. Thus there are an infinite number of solutions to the HF equations. Koopmans' also defined a unique solution for this case as the extreme values of the symmetric energy matrix $(\varepsilon_{nl,n'l})$. For these extreme values, the $1s$ orbital is the most bound orbital in the set of possible solutions, the $2s$ the orbital least bound, and the off-diagonal Lagrange multiplier is zero [52]. Thus, in HF calculations, it is customary to omit the rotations of orbitals of two filled subshells and their Lagrange multipliers, thereby implicitly setting the Lagrange multipliers to zero. But filled subshells are not the only case where the wave function remains invariant under rotation. Another well-known example is $1s2s\ ^3S$ [52]. Non-unique cases can be detected through rotation analysis in that, for such cases, $g = g' = 0$ and the Lagrange multiplier can be set to zero [105].

Compiled on 2016/01/23 at 13:08:13

3.5. Brillouin's theorem

The requirement that the "best" solution satisfy the stationary condition of Eq. (54) can be generalized to matrix elements of the Hamiltonian between CSFs or linear combinations of CSF. At this point it is important to keep in mind the nature of the perturbations of radial functions. In the Hartree-Fock approximation, the "best" wave function is the Hartree-Fock solution

$$\Psi^{\rm best} = \Phi^{\rm HF}(\gamma LS) \; .$$

When a single orbital is perturbed, the perturbations can be expressed in terms a complete basis $P_{n'l}(r)$, orthogonal to the occupied orbitals. Then the stationary condition for all δP_a will be satisfied if it is satisfied for every $\delta P_{nl} = \epsilon P_{n'l}$. This perturbation of the radial function, denoted by $nl \rightarrow n'l$ results in a perturbation of the CSF, $\Phi(\gamma LS)_{nl\rightarrow n'l}$. If we recall the construction of the CSF, and Eq. (38), it is clear that none of the spin-angular factors are affected. Thus, in $1s^2 2s$, for example only the CSF for the sub-shell containing orbital a (or nl) will be affected. Thus the perturbation of the Hartree-Fock $2s$-radial function, $P_{2s} \rightarrow P_{2s} + \epsilon P_{ns}$, leads to

$$\begin{aligned} &(r_1 r_2 r_3)^{-1} \left[P_{1s}(r_1) P_{1s}(r_2) \left[P_{2s}(r_3) + \epsilon P_{ns}(r_3)\right]\right] |ss(^1S)s \; ^2S\rangle \\ &\equiv \Phi^{\rm HF}(1s^2 2s \; ^2S) + \epsilon \; \Phi(1s^2 ns \; ^2S), \end{aligned} \tag{76}$$

so that, to first order in ϵ,

$$\begin{aligned} E(\epsilon) \quad &= \langle \Phi^{\rm HF}(1s^2 2s \; ^2S) | H | \Phi^{\rm HF}(1s^2 2s \; ^2S) + \epsilon \; \Phi(1s^2 ns \; ^2S) \rangle \\ &= E^{\rm HF} + 2\epsilon \; \langle \Phi^{\rm HF}(1s^2 2s \; ^2S) | H | \Phi(1s^2 ns \; ^2S) \rangle + \mathcal{O}(\epsilon^2) \; . \end{aligned} \tag{77}$$

Since the HF solution is stationary for this perturbation, it follows that

$$\langle \Phi^{\rm HF}(1s^2 2s \; ^2S) | H | \Phi(1s^2 ns \; ^2S) \rangle = 0, \; \forall \; n. \tag{78}$$

In this case, adding the $\Phi(1s^2 ns \; ^2S)$ to the HF wave function as a correction, would not further lower the energy and it is convenient to think of the HF wave function as already having included these CSFs.

The situation changes when orbitals are multiply occupied and the structure of $\tilde{\Phi}_{nl\rightarrow n'l}$ satisfying

$$\langle \Phi^{\rm HF}(\gamma LS) | H | \tilde{\Phi}_{nl\rightarrow n'l} \rangle = 0 \; , \tag{79}$$

in the general case, is more complex [106]. Consider $2p^3 \; ^2P^o$. We must first uncouple an orbital using Eq. (36) in order to have a single $2p$ coupled to an expansion over the parent $2p^2 \; LS$ terms where this expansion is determined by the CFPs. Expressing the perturbed wave function in terms of CSFs, the stationary condition requires that the Brillouin matrix element be zero, or

$$\langle \Phi^{\rm HF}(2p^3 \; ^2P^o) | H | \tilde{\Phi}_{2p\rightarrow np} \rangle = 0 \; . \tag{80}$$

In the present case, this is a matrix element between $2p^3 \; ^2P^o$ and a particular linear combination of CSFs $\Phi(2p^2(L'S')np \; ^2P^o)$, namely

$$\begin{aligned} &|\tilde{\Phi}_{2p\rightarrow np}\rangle = \\ &\sqrt{3}\left\{ -\sqrt{\frac{1}{2}} |2p^2(^3P)np \; ^2P^o\rangle - \sqrt{\frac{5}{18}} |2p^2(^1D)np \; ^2P^o\rangle + \sqrt{\frac{2}{9}} |2p^2(^1S)np \; ^2P^o\rangle \right\} \; , \end{aligned} \tag{81}$$

where the weights are the associated coefficients of fractional parentage (36). Thus the HF solution has included a particular combination of $2p^2 np$ CSFs but not each CSF

Compiled on 2016/01/23 at 13:08:13

exactly: adding the three CSFs separately, each with their own expansion coefficient, would lower the energy of the HF wave function.

When two orbitals a, b are subject to an orthogonality condition, the perturbation from a rotation must also have a zero interaction with the HF wave function [107, 108]. This perturbation comes from a pair of substitutions, namely $a \to b, b \to -a$. An excellent example is the excited state $1s2s\ ^1S$. A rotational perturbation produces a state proportional to $\{2s^2 - 1s^2\}/\sqrt{2}\ ^1S$. The stationary condition requires that the HF solution be such that

$$\left\langle \Phi(1s2s\ ^1S)|H|\frac{\{2s^2 - 1s^2\}}{\sqrt{2}}\ ^1S \right\rangle = 0.$$

This condition on the solution is difficult to satisfy without the use of rotational transformations. In general, when two open shells of the same symmetry are present, Brillouins theorem states that HF solutions have the property that the interaction between the HF solution and a specific linear combination of CSFs will be zero [109], implying that some average interaction been CSFs has been included in the approximation. We will show later that the $1s2s\ ^1S$ state and the perturbed linear combination of CSFs are degenerate in Z-dependent perturbation theory.

Brillouin's theorem states, in effect, that $\langle \Phi^{\rm HF}|H|\tilde{\Phi}\rangle = 0$ for a class of functions that can be related to the allowed perturbations for which the energy is stationary. The "annihilation" of Brillouin's matrix elements for fully variational solutions of the HF problem constitutes a useful property. It has been intensively used for testing the extension of the HF code to the f^N shell for general occupation numbers [85]. It is worthwhile to note that in the checking process, "accidental" zeros characterizing the Hartree-Fock solution of Lanthanides in their ground state and appearing in $4f \to nf$ Brillouin's matrix elements were discovered and remain unexplained, even after exploring the use of an isospin basis [110, 111].

3.6. Solution of the HF equations

With these theorems in mind, given an initial estimate for all the occupied radial functions, solutions to the HF equations of Eq. 68 can be obtained by an iterative process referred to as the self-consistent field (SCF) method, namely:

while *not converged* **do**
  Orthogonalize all orbitals;
  Rotate orbitals for a stationary energy, if necessary;
  Compute diagonal and off-diagonal energy parameters;
  for *each orbital, in turn* **do**
    Compute the direct $Y(a;r)$ and exchange $\bar{X}(a;r)$ potential;
    Solve the differential equation for orbital a;
    Update the orbital;
  end
end

Very efficient methods solve the differential equations by using finite differences based on a discrete representation of the radial functions on a logarithmic mesh. Details can be found in [52, 105]. Essentially, in every iteration, the method improves the radial function. This is done by matching the solutions from outward integration and inward integration. Since the differential equations for excited states may be

Compiled on 2016/01/23 at 13:08:13

the same as for a lower state, the adjustment process needs to take into account the desired eigenstate. Node counting is used in the numerical HF program, taking into account the possibility that the rotation of orbitals may have introduced additional nodes that need to be ignored, thereby making node counting somewhat of an art. But the SCF process does not guarantee convergence. A well-known example which starts with large oscillations is F $2p^5\ ^2P^o$: if the $2p$ estimated orbital is too contracted, the screening of the nucleus will be too large, and the next estimate will be too extended. "Accelerating" parameters may be introduced that actually dampen the rate of change thereby damping the oscillations in the change of the orbitals and speeding convergence [56].

The accuracy of the solution of the Hartree-Fock equation can be assessed through the virial theorem [57] which states that the ratio of the potential energy relative the kinetic energy is exactly -2.0.

3.7. Dirac-Hartree-Fock equations

The Dirac-Hartree-Fock (DHF) equations are similar to the non-relativistic equations for a single CSF except for some differences in the details. By definition, HF and DHF are methods applied to a single CSF either in LS or jj-coupling. In many cases, the two are equivalent but in others there is a difference. For example, the $2p^4\ ^1D$ case in non-relativistic theory becomes $0.8258\ (2p_-2p_+^3)+0.5648\ (2p_-^2\,2p_+^2)$ in jj-coupling and Dirac theory. Therefore the equivalent of the HF wave function is no longer a single CSF and needs to be treated as part of a multiconfiguration approximation discussed in the next section.

The relativistic extension of the HF approach to the DHF approach is to apply the variational principle to the energy functional

$$\mathcal{F}(\{P\},\{Q\};\gamma J) = \langle \gamma J|\mathcal{H}_{DC}|\gamma J\rangle + \sum_{a,b}\delta(\kappa_a,\kappa_b)\lambda_{ab}\mathcal{C}_{ab}\ \ , \tag{82}$$

where $|\gamma J\rangle$ is a single CSF (50), and $\mathcal{H}_{DC}$ is the Dirac-Coulomb Hamiltonian (8). Lagrange multipliers are introduced for each radial orthonormality constraint within each κ-space, namely

$$\mathcal{C}_{ab} \equiv \int \left[P_a(r)P_b(r) + Q_a(r)Q_b(r)\right] dr - \delta_{n_a,n_b} = 0. \tag{83}$$

The matrix element for the total energy for the Dirac-Coulomb Hamiltonian (8) can be expressed in terms of spin-angular coefficients and radial integrals,

$$\langle \gamma J|\mathcal{H}_{DC}|\gamma J\rangle = \sum_a w_a I(a,a) + \sum_{abk}\left[f_{abk}F^k(ab) + g_{abk}G^k(ab)\right] \tag{84}$$

The one-body interaction gives rise to the spin-angular coefficients that reduce to occupation numbers w_a and to the $I(a,a)$ integrals where (in the general case)

$$\begin{aligned} I(a,b) = \delta(\kappa_a,\kappa_b)\int_0^\infty \Bigg\{ & P_a(r)V_{nuc}(r)P_b(r) - cP_a(r)\left(\frac{d}{dr} - \frac{\kappa}{r}\right)Q_b(r) \\ & + c\,Q_a(r)\left(\frac{d}{dr} + \frac{\kappa}{r}\right)P_b(r) + Q_a(r)\left(V_{nuc}\,(r) - 2c^2\,\right)Q_b(r)\Bigg\}\, dr. \end{aligned} \tag{85}$$

The two-body interaction gives rise to the spin-angular coefficients f_{abk}, g_{abk} and to the $F^k(ab) = R^k(ab,ab)$ and $G^k(ab) = R^k(ab)$ integrals. The latter are special cases

Compiled on 2016/01/23 at 13:08:13

of the relativistic Slater integrals,

$$R^k(ab,cd) = \int_0^\infty \left[P_{n_a\kappa_a}(r)P_{n_c\kappa_c}(r) + Q_{n_a\kappa_a}(r)Q_{n_c\kappa_c}(r)\right] \frac{1}{r} Y^k(bd;r)dr. \qquad (86)$$

The relativistic DHF Y^k-functions are defined by

$$Y^k(ab;r) = r\int_0^\infty \frac{r_<^k}{r_>^{k+1}} \left[P_{n_a\kappa_a}(s)P_{n_b\kappa_b}(s) + Q_{n_a\kappa_a}(s)Q_{n_b\kappa_b}(s)\right] ds. \qquad (87)$$

The spin-angular coefficients appearing in (84) can be evaluated using algebraic expressions for matrix elements adapted for spin-angular integrations in jj coupling, involving the calculation of reduced coefficients of fractional parentage and completely reduced matrix elements of double tensors [112, 113].

From this expression it is possible to derive the DHF equations from the usual variational argument [62]

$$w_a \begin{bmatrix} V(a;r) & -c\left[\frac{d}{dr} - \frac{\kappa}{r}\right] \\ c\left[\frac{d}{dr} + \frac{\kappa}{r}\right] & V(a;r) - 2c^2 \end{bmatrix} \begin{bmatrix} P_a(r) \\ Q_a(r) \end{bmatrix} = \sum_b \varepsilon_{ab}\, \delta_{\kappa_a,\kappa_b} \begin{bmatrix} P_b(r) \\ Q_b(r) \end{bmatrix}, \qquad (88)$$

where $V(a;r) = \left(V_{nuc} + Y(a;r) + \bar{X}(a;r)\right)$. In this expression, V_{nuc} is the effective electron-nucleus potential at radius r taking into account the finite size of the nuclear charge distribution through a uniform or a Fermi distribution of the charge, $Y(a;r)$ is the direct potential, and $\bar{X}(a;r)$ contains the exchange contributions in integro-differential form as described in the HF method.

Koopmans' and Brillouin's theorems apply to the DHF solution as well. One major difference compared with LS non-relativistic theory is that CSFs in jj-coupling have more subshells. In fact, non-relativistic single CSF approximations are frequently multiconfiguration expansions in Dirac theory, a topic discussed in the next section.

4. The Multiconfiguration Wave Functions

The single CSF approach described in the previous section is based on an independent particle model, where the electrons are assumed to move in an average, central field of the other electrons and the nucleus. In this approach we do not start by defining a detailed form for these potentials, just the fact that they define the form of our wave functions, as linear combination of products of spin-orbitals (5) or (10). We then develop the HF and DHF method by assuming this form of the orbitals. To take into account corrections to the independent particle model is, by definition, to include electron *correlation* which we will discuss in a later section. Here we just observe that a "straight-forward" approach would be to represent the Atomic State Function (ASF), not any longer as a single CSF, but as a Multi-configuration (MC) function expanded in terms of a basis of, say M, CSFs;

$$\Psi = \sum_{\alpha=1}^{M} c_\alpha \Phi_\alpha. \qquad (89)$$

In our definition of an MC approach, we assume two "processes":

(i) the determination of the c_α coefficients, or weights, of the CSFs. We will refer to this as the Configuration Interaction (CI) process, and

(ii) the determination of the orbitals, as an extension to the HF or the DHF method.

Let us start with the CI process.

Compiled on 2016/01/23 at 13:08:13

4.1. Configuration interaction

In a "pure" CI approach, only the expansion coefficients in (89) are variational parameters and can be determined by the Rayleigh-Ritz method. The stationary condition then leads to the eigenvalue problem

$$(\mathbf{H}^M - E^M\mathbf{I})\mathbf{c}^M = 0\ , \tag{90}$$

where we assume an orthonormal orbital basis. In fact there are M eigenvalues and eigenvectors, often referred to as eigenpairs. If the m^{th} eigenvalue, E_m^M is the total energy of the desired state, then the associate normalized eigenvector $\mathbf{c}_m^M$ defines the expansion coefficients for the state. The $M \times M$ matrix $\mathbf{H}^M = (H_{\alpha\beta})$ is called the "interaction matrix" and has elements

$$H_{\alpha\beta} = \langle\Phi_\alpha|\mathcal{H}|\Phi_\beta\rangle\ . \tag{91}$$

As stated in the introduction, we are aiming for a systematic approach, where we include a set of CSFs of increasing size to improve our approximate ASF. An essential foundation for this is the Hylleraas-Undheim-MacDonald (HUM) theorem [114, 115], which states the following relationship for the eigenvalues when the size of the matrix increases from M to $M+1$, namely

$$\ldots E_{m-1}^M \le E_m^{M+1} \le E_m^M \ldots\ . \tag{92}$$

In other words, the eigenvalues of the matrix of size M interlace those of size $M+1$. The implication of this is that when the basis set is increased by including an additional CSF of the same symmetry, we are approaching the exact solution for the energy from above. It then follows that the m^{th} eigenvalue is an upper bound for the m^{th} *exact* solution of the wave equation for the Hamiltonian operator $\mathcal{H}$, provided the matrix size is at least $M \ge m$. To be even more explicit, if the energies are bounded from below as in non-relativistic theory, the HUM theorem shows that the variational method is a minimization method not only for ASFs lowest in their symmetry, but also for excited states as long as the basis includes the CSFs needed for the lower states. As an example, if we apply the HUM theorem to $E^{\rm HF}(1s2s\ ^1S)$ states in He-like systems, then this energy calculation for this matrix of size $M = 1$, is an upper bound to the energy of the *ground* state. In order to obtain a wave function whose energy is an upper bound to the exact $1s2s\ ^1S$ energy, it is necessary to have an expansion over a basis that includes the $1s^2\ ^1S$ CSF as well as $1s2s\ ^1S$ so that the desired solution is the second one with $M \ge 2$. The calculation of the wave function of the $1s2s\ ^1S$ state has a long history [116, 117].

The HUM theorem has implications for variational calculations for hole states such as $1s2s^22p^6$, for example. The $1s^22s2p^6$ CSF needs to be included in the expansion in order for the hole state to be the second eigenstate and an upper bound to the exact solution.

4.1.1. The two-by-two CSF example The CI method is frequently used in atomic physics, and has become a metaphor for "interacting configurations" that represent correlation. To understand some of its implications it is valuable to investigate the simplest case of $M = 2$, to see what differs from the single-configuration approach. In this case the matrix eigenvalue problem is

$$\begin{pmatrix} H_{11} & H_{12} \\ H_{21} & H_{22} \end{pmatrix} \begin{pmatrix} c_1 \\ c_1 \end{pmatrix} = E \begin{pmatrix} c_2 \\ c_2 \end{pmatrix}, \tag{93}$$

Compiled on 2016/01/23 at 13:08:13

with $H_{21} = H_{12}$, since we are dealing with Hermitian operators. The eigenvalues for this problem are roots of the quadratic polynomial obtained from the secular equation

$$\det |\mathbf{H} - E\mathbf{I}| = 0. \tag{94}$$

The two real roots E_+ and E_-, of this equation are [87]

$$E_\pm = \frac{H_{11} + H_{22}}{2} \pm \frac{1}{2}\sqrt{(H_{22} - H_{11})^2 + 4H_{12}^2}\,, \tag{95}$$

and the corresponding eigenvectors

$$\begin{pmatrix} c_1^\pm \\ c_2^\pm \end{pmatrix} = \frac{1}{\sqrt{1 + r\pm^2}} \begin{pmatrix} +1 \\ r_\pm \end{pmatrix} = \frac{1}{\sqrt{1 + r\mp^2}} \begin{pmatrix} r_\mp \\ -1 \end{pmatrix}\,, \tag{96}$$

with

$$r_\pm = \frac{-1}{r_\mp} = \frac{H_{22} - H_{11}}{2H_{12}} \pm \sqrt{\left(\frac{H_{22} - H_{11}}{2H_{12}}\right)^2 + 1}\,. \tag{97}$$

Note that one eigenvalue is above $\max(H_{11}, H_{22})$ while the other is below $\min(H_{11}, H_{22})$. Due to the fact that the trace is conserved ($H_{11} + H_{22} = E_- + E_+$) it is clear that the interaction term ($H_{12} = H_{21}$) produces an apparent mutual repulsion of the two energy levels.

Two interesting cases may be be considered

- the off-diagonal interaction H_{12} can be considered as a perturbation of the diagonal energies when $|2H_{12}/(H_{22} - H_{11})| \ll 1$,
- the diagonal energies are "nearly degenerate" ($|(H_{22} - H_{11})/2H_{12}| \ll 1$).

In the former, assuming without loss of generality that $H_{11} < H_{22}$ and expanding the square roots of (95) and (97) in binomial series, one finds

$$E_- \approx H_{11} - \frac{H_{12}^2}{H_{22} - H_{11}}\,, \quad E_+ \approx H_{22} + \frac{H_{12}^2}{H_{22} - H_{11}}\,, \tag{98}$$

and, for the small components of the corresponding eigenvectors

$$c_2^- \approx -\frac{|H_{12}|}{H_{22} - H_{11}}\,, \quad c_1^+ \approx \frac{|H_{12}|}{H_{22} - H_{11}}\,. \tag{99}$$

For the second case, the most spectacular scenario occurs in the degenerate case ($H_{11} = H_{22}$) for which the two eigenvectors are mixed 50-50% with ($|c_1^\pm|^2 = |c_2^\pm|^2$) for any non-zero H_{12} matrix element.

There are many near degeneracies in atomic spectra. An example is the high-lying perturber $3s3p^5\ ^3P^o$ CSF in the sulfur iso-electronic sequence which interacts with the $3s^23p^3(^2D)nd\ ^3P^o$ Rydberg series CSFs. As the nuclear charge of the atomic system increases [118] the perturber descends into the lower region of the spectrum and the energies of the two components of the wave function change order. As a result there may be "short-range" interactions in the presence of level crossings at selected values of Z and the order of the dominant component changes and hence, also the label [119]. However, the energy of solutions to the wave equation are continuous functions of Z and plots of the lowest energy of a given symmetry, the second lowest, etc., are continuous functions with an anti-crossing at the point of degeneracy. A unique identification of an ASF is a position number (POS) and symmetry. (Do we need to introduce POS?)

Compiled on 2016/01/23 at 13:08:13

4.2. The MCHF method

Multiconfiguration methods, MCHF or MCDHF, differ from CI methods in that both the expansion coefficients and the radial functions are varied for a stationary energy. The procedures are the same as for the single CSF wave function and many of the properties are similar except for some differences. Though the single configuration case is a subset of the multiconfiguration case, here we will focus on the differences.

In the MCHF method the normalized atomic state wave function (ASF) is expanded in a basis set of M CSFs,

$$\Psi(\gamma LS) = \sum_{\alpha=1}^{M} c_\alpha \Phi(\gamma_\alpha LS), \text{ where } \sum_\alpha c_\alpha^2 = 1, \tag{100}$$

and the associated energy becomes

$$\begin{aligned} E^{\mathrm{MCHF}} &= \langle \Psi | \mathcal{H}_{NR} | \Psi \rangle = \sum_{\alpha\beta} c_\alpha c_\beta \langle \Phi_\alpha | \mathcal{H}_{NR} | \Phi_\beta \rangle \\ &= \sum_\alpha c_i^2 H_{\alpha\alpha} + \sum_{\alpha \neq \beta} c_\alpha c_\beta H_{\alpha\beta} \ . \end{aligned} \tag{101}$$

The diagonal matrix elements for the energy can be expressed as linear combinations of one-electron integrals $I(a,a)$ and two-electron Slater integrals $F^k(ab)$ and $G^k(ab)$, as in the HF case (see (56) and (58)), but off-diagonal matrix elements introduce one-electron integrals $I(a,b)$ and Slater integrals $R^k(ab,cd)$ with symmetries different from the $F^k(ab) = R^k(ab,ab)$ (direct) and the $G^k(ab) = R^k(ab,ba)$ (exchange) symmetry. For example, $\langle 3p^2\ {}^1D | \mathcal{H}_{NR} | 3s3d\ {}^1D \rangle = 2\sqrt{5/3}\ R^1(3p3p, 3s3d)$. Then the energy functional has the form

$$\langle \Psi | \mathcal{H}_{NR} | \Psi \rangle = \sum_{ab} t_{ab} I(a,b) + \sum_{abcd;k} v_{abcd;k} R^k(ab,cd) \tag{102}$$

where

$$t_{ab} = \sum_{\alpha\beta} t_{ab}^{\alpha\beta} c_\alpha c_\beta \quad \text{and } v_{abcd;k} = \sum_{\alpha\beta} v_{abcd;k}^{\alpha\beta} c_\alpha c_\beta \tag{103}$$

are contributions from all the interactions between CSFs. The coefficient $t_{aa}^{\alpha\alpha}$ is the occupation of the orbital a in CSF α and $t_{aa} = w_a$ is the generalized occupation number of an orbital a in analogy with the HF notation. Similarly, $v_{abcd;k}^{\alpha\beta}$ is the contribution to the energy of a given Slater integral.

As in the derivation of the HF equations from the variational principle [52], Lagrange multipliers are introduced for each constraint $\mathcal{C}_{ab}$ defining the energy functional

$$\mathcal{F}(\{c\},\{P\};\gamma LS) = \langle \Psi | \mathcal{H}_{NR} | \Psi \rangle + \sum_{ab} \delta(l_a, l_b) \lambda_{ab} \mathcal{C}_{ab} \tag{104}$$

where $\mathcal{C}_{ab}$ is the orthonormality constraint (63). Both the expansion coefficients c and the radial functions P are varied.

For a given set of radial functions $\{P_{nl}(r)\}$, the total energy is optimized through the variation of the expansion coefficients as in the CI method, leading to the matrix eigenvalue problem,

$$\mathbf{Hc} = E\mathbf{c} \tag{105}$$

with many solutions. Only one eigenvector is the desired eigenvector, not necessarily the lowest and this vector defines the expansion coefficients.

Compiled on 2016/01/23 at 13:08:13

Table 2. Total energies in E_h for $2p^4\ {}^3P$ ASF in oxygen illustrating the role of Brillouin's theorem as a function of the method on the total energy and the expansion coefficients: 1) HF, 2) MCHF for $\{2p^4, 2p^3 3p\}$, and 3)$\{2p^4, 2p^3 3p, 2p^2 3p^2\}$. In 2a) and 3a) the $1s, 2s, 2p$ are fixed and only $3p$ varied, whereas in 2b) and 3b) both $2p$ and $3p$ are varied allowing orbital rotations.

	Varied	Total	Expansion Coefficients			
		Energy	$2p^4$	$2p^3(^2P)3p$	$2p^3(^2D)3p$	$2p^3(^4S)3p$
1)	all	-74.809398	1.0000			
2a)	$3p$	-74.812490	0.9977	0.0379	-0.0154	-0.0532
2b)	$2p, 3p$	-74.841396	0.9179	-0.1669	0.2426	-0.2659
3a)	$3p$	-74.844914	0.9942	0.0209	-0.0072	-0.0301
3b)	$2p, 3p$	-74.845367	0.9936	0.0110	0.0065	-0.0443

For a given set of mixing coefficients $\{c_\alpha\}$, the stationary condition with respect to a variation in the radial functions, $\delta P_a(r)$, leads to a system of coupled differential equations

$$w_a \left[-\frac{1}{2}\frac{d^2}{dr^2} - \frac{Z}{r} + \frac{l_a(l_a+1)}{2r^2} + Y(a,r) + \bar{X}(a,r) \right] P_a(r) = \sum_b \varepsilon_{ab} P_b(r), \qquad (106)$$

similar in form to the HF equations (68). What differs are the types on integrals that may occur in the energy expression. Slater integrals of the symmetry $R^k(ab, ab)$ again contribute to the direct potential $Y(a, r)$ through $Y^k(bb, r)/r$ functions. All other $R^k(ab, cd)$ integrals contribute to $\bar{X}(a, r)$ through $Y^k(bd, r)P_c(r)/r$ functions. Also included in $\bar{X}(a, r)$ are contributions from $I(a, b)$ integrals where $b \neq a$. Again, for each orbital angular momentum, there is a matrix (ε_{ab}) arising from the orthogonality constraints [52].

4.2.1. Brillouin's theorem for multiconfiguration solutions Properties of the HF equations can be extended to the MCHF equations, with some qualifications.

The generalized Brillouin's theorem is not nearly as important as in HF when a given orbital occurs in many CSFs. If $\Psi_{nl}^{\rm MCHF}$ is the portion of the ASF (complete with expansion coefficients) that contains the orbital nl and $\Psi_{nl\to n'l}^{\rm MCHF}$ represents the function obtained through the $nl \to n'l$ substitutions that themselves may require expansions in terms of CFP's when an orbital is multiply occupied, then the following holds:

$$\langle \Psi_{nl}^{\rm MCHF} | \mathcal{H}_{NR} | \Psi_{nl\to n'l}^{\rm MCHF} \rangle = 0. \qquad (107)$$

Thus the included interactions may only apply in a broad average sense.

Table 2 shows the role of Brillouin's Theorem in HF and MCHF calculations. For the HF calculation, (79) states that the interaction between $2p^4$ and a specific linear combination of the $2p^3 3p$ CSFs has a zero matrix element but by adding the CSFs explicitly into a CI calculation, the energy is reduced significantly. Varying both $2p$ and $3p$ reduces the total energy more but, at the same time, the rotations that enter into such a calculation have a noticeable effect on the expansion coefficients. In calculation 3a) and 3b), CSFs such as $2p^2 3p^2$ are also present. These CSFs are part of Brillouin's theorem for calculation 2b). Varying both $2p$ and $3p$ again allows for orbital rotations but the energy reduction is now considerably less and the expansion

coefficients for $2p^3 3p$ CSFs are not greatly changed. Not given in this table are the expansion coefficients of $2p^2 3p^2$. Thus, in general, Brillouin's theorem is not significant for larger multiconfiguration expansions.

But it may still have a significant effect in some small cases. An example is the interaction of $|3s3p^6\ ^2S\rangle$ with the $|3s^2 3p^4 nd\ ^2S\rangle$ continuum in Cl. In the HF approximation, the former is located in the continuum but with the introduction of the single $|3s^2 3p^4 3d\ ^2S\rangle$ CSF into the wave function expansion, the MCHF $3d$ orbital has included the effect of both the interaction with the continuum states and the bound states. This $3d$ orbital has a mean radius similar to that of the $3p$ orbital [120]. It was confirmed that the MCHF results agreed with perturbation theory only when the latter included both continuum and bound states. In this case, the interaction with the continuum lowered the energy of the state into the bound spectrum and the $3d$ orbital became a bound orbital approaching zero at large r. This is an example where the summation over continuum states may cancel at large r so that the state does not "decay" into the continuum.

4.2.2. Uniqueness of the multiconfiguration solutions For multiconfiguration expansions, rotational analysis for detecting a non-unique solution [105] is usually not of sufficient benefit, to justify the needed computational effort. The probability of a non-unique solution often decreases when many different CSFs of different symmetries are included except for a certain class of expansions and modifications can be made to the expansion so that equations have a unique solution.

Well-known cases for which the radial functions are not unique are complete active space (CAS) expansions [121]. Consider an ASF for $1s^2\ ^1S$ and the orbital set $\{1s, 2s\}$ of the same symmetry. Let the CSF basis be the set of all two-electron ^1S CSFs that can be constructed from these orbitals, namely $\{1s^2, 1s2s, 2s^2\}\ ^1S$. Any rotational transformation of the orbital set changes the expansion coefficients of the ASF, but leaves the wave function and its energy invariant. Without a unique solution, a computational process for a solution may still converge (if nodal properties are relaxed) but will depend on the initial estimates. Computationally, it is desirable to have a well-defined solution. Koopmans' theorem for similar situations in the HF case sets the off-diagonal Lagrange multiplier to zero, but this does not always work well for a CAS solution. Essentially, with this CAS expansion, there is a degree of freedom in the expansion. Much more can be gained by using the degree of freedom to set one of the expansion coefficients to zero or, equivalently, eliminating a CSF from the expansion. If the desired solution had been for $1s2s\ ^1S$, then clearly $2s^2$ should be eliminated so our computed solution would be an upper bound to the second exact solution of the Hamiltonian. For such a solution, the generalized Brillouin's theorem states that the interaction between Ψ^{MCHF} and perturbation obtained by rotating the $1s, 2s$ orbitals is zero, which in this case is easier to confirm through computation than direct analysis, and the energy is the same as the CAS energy.

But what should be eliminated if the desired solution is the ground state? In this case the HUM theorem is not helpful.

Suppose the orbital set is the $\{1s, 2s, \ldots ms\}$ set so that the CSF basis consists of all $\{nsn's\ ^1S\}$ CSFs, with $n, n' \leq m$. The expansion over this basis is a two-electron partial wave since every CSF has the same $|ss'\ ^1S\rangle$ spin-angular factor and could be

Compiled on 2016/01/23 at 13:08:13

written as

$$\Psi^{l=0}(1s^2\ ^1S) = \left(\sum_{n,n'} c_{nn'} R_{ns}(r_1) R_{n's}(r_2)\right) |ss'\ ^1S\rangle >, \tag{108}$$

where $R_{nl}(r) = P_{nl}(r)/r$ and $c_{nn'} = c_{n'n}$. The above radial factor for the partial wave can be expressed in matrix vector form. Let $\mathbf{C}$ be the symmetric matrix $c_{nn'}$, and $\mathbf{R}(\mathbf{r})$ the row vector $\{R_1(r), R_2(r), \ldots, R_m(r)\}$. Then the radial factor becomes

$$\left(\sum_{n,n'} c_{nn'} R_{ns}(r_1) R_{n's}(r_2)\right) = \mathbf{R}(\mathbf{r_1})\ \mathbf{C}\ \mathbf{R}(\mathbf{r_2})^t. \tag{109}$$

Since $\mathbf{C}$ is symmetric, there exists a unitary transformation that will diagonalize the matrix of expansion coefficients so that the partial wave has the form

$$\Psi^{\mathrm{MCHF}}(1s^2\ ^1S) = \sum_n c_n\ |ns^2\ ^1S\rangle. \tag{110}$$

The process can be extended to other symmetries so that

$$\Psi^{\mathrm{MCHF}}(1s^2\ ^1S) = \sum_l \sum_n c_{nl}\ |nl^2\ ^1S\rangle. \tag{111}$$

The orbitals of this "reduced form" of the wave function are also called the "natural" orbital expansion [52, 122] and are the ones that diagonalize the density matrix [123, 124]. It is the form obtained by using each of the $(m \times (m-1))/2$ degrees of freedom toward eliminating the "off-diagonal" CSFs.

The forms of these orthogonal transformations depend on the spin-angular symmetry of the different partial waves [122]. For a $^1P^o$ two-electron system, the set of partial waves have the symmetry $\{sp, pd, df, \ldots\}$. In this case the radial transformations for reducing the $nsn'p$ expansion to $ns(n+1)p$ expansions differ from the radial transformations reducing the $npn'd$ expansion to $np(n+1)d$. For this reason, the reduced forms cannot be used simultaneously in both sp and pd subspaces, unless the sets of p-orbitals involved in the two couplings are allowed to differ. This was one of the original motivations for implementing non-orthogonal orbitals that preserve the othonormality of CSFs within a partial wave [125].

For a given active orbital set, the size of a CAS expansion grows dramatically with the number of electrons and "Restricted Active Space" (RAS) wave functions [126] should be built. For nominal two-electron atoms such as alkaline-earth atoms and atoms of the IIB group of the periodic table, multiconfiguration expansions can be generated by restricting the excitations to the outer valence shells (*i.e.* no hole in the core), and using the reduced forms with non-orthogonal orbitals to include valence correlation [127, 128].

When the generalized occupation is small, the associated radial function is quite different from the normal "spectroscopic" (hydrogenic) orbital. Koopmans' theorem also has a different interpretation. Consider the case

$$\Psi^{\mathrm{MCHF}}(1s^2\ ^1S) = c_1|1s^2\ ^1S\rangle + c_2|4f^2\ ^1S\rangle \tag{112}$$

where no orthogonality constraints are present. By substituting the expressions for the matrix elements into (101), the expression for the total energy becomes the sum

Compiled on 2016/01/23 at 13:08:13

of integrals with coefficients weighted by expansion coefficients. For our example, it is easy to show that

$$\begin{aligned} \varepsilon_{1s1s} &= E^{\rm MCHF}(1s^2\ ^1S) - \bar{E}(1s) + c_1^2\ \langle 1s^2\ ^1S|1/r_{12}|1s^2\ ^1S\rangle \\ \varepsilon_{4f4f} &= E^{\rm MCHF}(1s^2\ ^1S) - \bar{E}(4f) + c_2^2\ \langle 4f^2\ ^1S|1/r_{12}|4f^2\ ^1S\rangle \end{aligned} \tag{113}$$

where $\bar{E}(nl)$ is the energy when the nl orbital has been removed (or set to zero). In the present example for He I, $c_2 = 0.005766$, and $4f^2$ clearly is a correction to the $1s^2\ ^1S$ ASF, lowering its total energy by 0.00066 E_h. But this $4f^2\ ^1S$ CSF is very different from a HF CSF. In fact, $H_{22} = 17.0166\ E_h$, which is well into the positive energy continuum although the $4f$ orbital is bound.

4.2.3. Solution of the MCHF equations Because the equations for the expansion coefficients and the radial functions are coupled, the MCHF equations are solved by the MC_SCF process, similar to the SCF except that, after orthogonalization of the orbital set, the interaction matrix needs to be computed and the desired eigenvectors determined. For solving large CI problems, the ATSP2K code uses an approach based on the Davidson method [129] with robust preconditioning [130]. This is an iterative method based entirely on matrix-vector multiplication, requiring an initial estimate of the desired solution. Initially, when no estimates are available, approximate values can be determined by diagonalizing a small matrix. After that, when the current estimate is used as a starting value for the Davidson algorithm as the MC_SCF iteration converges, improved eigenvectors can be obtained with only a few (2-3) matrix-vector multiplies. Sparse matrix methods are used for representing the interaction matrix since possibly only 10% of the matrix or less may be non-zero.

The differential equations are solved using finite difference methods based on a discrete representation of the radial functions on a logarithmic mesh. Details can be found in [52, 105]. For selecting the solution of a given differential equation, node counting of the radial function is applied to the spectroscopic orbitals that are defined as those occupied in the single configuration HF approximation, or more generally, orbitals that have a generalized occupation number of 0.5 or greater. In technical terms node counting amounts to guiding the solution of the differential equation in such a way that radial functions have the same node structure as the corresponding hydrogen-like function provided small amplitudes in the tail are ignored that result from the rotation of orbitals. No node constraint needs to be imposed on the orbitals that are unoccupied in the HF approximation.

4.2.4. Extended MCHF methods The MCHF method can also be used to simultaneously obtain wave functions for many states. If all are of the same symmetry, the states may require many eigenvalues and eigenvectors of the same interaction matrix, or they may have different symmetries or parities, in which case different interaction matrices are needed. The variational principle is then applied to a weighted linear combination of functionals of the individual states and the energies and expansions coefficients are obtained as the corresponding eigenvalues and eigenvectors of the Hamiltonian matrix for the given symmetry [54]. This method is extremely useful for Breit-Pauli calculations, discussed next.

Compiled on 2016/01/23 at 13:08:13

4.3. Breit-Pauli wave functions

For light atoms, where relativistic effects are expected to be small, an orthonormal orbital basis from an ordinary or extended MCHF calculation may be used in combination with the CI method and the Breit-Pauli Hamiltonian, $\mathcal{H}_{BP}$ (25). This method has produced many J-dependent energy levels [131] in good agreement with observation. An example of the use of the CI method is given by the Breit-Pauli calculations [131] in which the non-relativistic Hamiltonian used for optimizing the orbitals in the MCHF approach is corrected by the inclusion of the BP relativistic operators (25). The CSF basis is extended to allow LS-term mixings for a given J and parity. The ASF is then an expansion over a set of CSFs (45),

$$\Psi(\gamma J) = \sum_{LS} \sum_{\alpha=1}^{M_{LS}} c_\alpha^{LS}\, \Phi(\gamma_\alpha LSJ), \text{ where } \sum_{LS} \sum_{\alpha} (c_\alpha^{LS})^2 = 1, \tag{114}$$

in which the $\mathbf{L} + \mathbf{S} = \mathbf{J}$ angular momentum coupling (37) is realized for each term symmetry. Here M_{LS} is the length of the expansion for a given LS term.

The evaluation of the Breit-Pauli operators appearing in (25) involves a large variety of radial integrals, as illustrated in [132, 133, 134, 135]. The two-body terms $\mathcal{H}_{SS}$ and $\mathcal{H}_{SOO}$ are not straight forward leading to many radial integrals. The complexity of the two-body $\mathcal{H}_{OO}$ operator however, exceeds those of $\mathcal{H}_{FS}$, increasing the computer time required to evaluate an interaction matrix. Thus, it has been customary to omit the orbit-orbit effect from energy spectrum calculations. The theory used to compute the interaction matrix assumes that *all* the CSFs are defined in terms of a single orthonormal set of orbitals. The extended MCHF method assures that this condition is met and has been used successfully to compute many levels of the Na-like to Ar-like sequences for nuclear charges up to $Z = 30$ [136].

4.3.1. Complete degeneracies When relativity is treated in the Breit-Pauli approximation, the relativistic corrections are included in the configuration interaction step with orbitals obtained from non relativistic HF/MCHF calculations. The LS-mixing can be dramatic when terms lie close to each other, or are accidentally degenerate. Complete degeneracies may occur when the two different term energy expressions are identical, i.e., they will be the same for all radial functions. For example, a strong relativistic mixing occurs between $2p^5 3d\ ^3D_2^o$ and $2p^5 3d\ ^1D_2^o$ due largely to the spin-orbit operator, as observed in the study of the Ne-like spectra [136]. A systematic analysis of the energy expressions shows that singlet-triplet term-degeneracies occur not only for $p^5 l\ ^1(L = l),\ ^3(L = l))$ but also for some singlet and triplet terms arising from the $l^{4l+1}l'$ configurations, as reported in Table 3.
In all these cases, strong relativistic mixing is expected for $J = L$. Note that if a degeneracy is found for some terms of $l^{4l+1}l'$, the complete degeneracy also holds for the same terms arising from $l'^{4l'+1}l$. This can be explained through the spin-quasispin exchange.

4.4. The MCDHF method

The relativistic extension of the MCHF approach is to define the ASF as an expansion over a set of jj-coupled relativistic CSFs (52),

$$\Psi(\gamma J) = \sum_{\alpha=1}^{M} c_\alpha \Phi(\gamma_\alpha J), \text{ where } \sum_{\alpha} c_\alpha^2 = 1, \tag{115}$$

Compiled on 2016/01/23 at 13:08:13

Table 3. Cases of complete degeneracies of singlet and triplet terms of $l^{4l+1}l'$ configurations

p^5p'	$(^1P,\ ^3P)$	d^9p	$(^1D,\ ^3D)$	$f^{13}p$	$(^1F,\ ^3F)$
p^5d	$(^1D,\ ^3D)$	d^9d'	$(^1P,\ ^3P)$	$f^{13}d$	$(^1D,\ ^3D)$
		d^9d'	$(^1F,\ ^3F)$	$f^{13}d$	$(^1G,\ ^3G)$
p^5f	$(^1F,\ ^3F)$	d^9f	$(^1D,\ ^3D)$	$f^{13}f'$	$(^1P,\ ^3P)$
		d^9f	$(^1G,\ ^3G)$	$f^{13}f'$	$(^1F,\ ^3F)$
				$f^{13}f'$	$(^1H,\ ^3H)$

and the energy functional

$$\mathcal{F}(\{c\},\{P\},\{Q\};\gamma J) \equiv \langle\Psi|H_{DC}|\Psi\rangle + \sum_{ab}\delta\kappa_a,\kappa_b\lambda_{ab}\mathcal{C}ab \tag{116}$$

as the expression for relativistic energy using the Dirac-Coulomb Hamiltonian (8). Lagrange multipliers are introduced for constraining the variations in the one-electron functions $(\delta P_{n\kappa},\delta Q_{n\kappa})$ to satisfy the constraint (83), that guarantees the orthonormality of the one-electron functions and of the CSFs.

The energy functional of (115) with the Dirac-Coulomb Hamiltonian (8) can be expressed in terms of spin-angular coefficients and radial integrals,

$$\langle\Psi|\mathcal{H}_{DC}|\Psi\rangle = \sum_{ab} t_{ab}I(a,b) + \sum_{abcd;k} v^k_{abcd}R^k(ab,cd), \tag{117}$$

where

$$t_{ab} = \sum_{\alpha\beta} t^{\alpha\beta}_{ab}, \quad v_{abcd;k} = \sum_{\alpha\beta} v^{\alpha\beta}_{abcd;k} \tag{118}$$

are contributions from all the interactions between CSFs. The one-body interactions give rise to the spin-angular coefficients t_{ab} and the $I(a,b)$ integrals defined by (85) and the two-body interactions to the spin-angular coefficients v^k_{abcd} and to the relativistic Slater integrals $R^k(ab,cd)$ defined by (86) and (87).

The coefficient of $I(a,a)$, namely $w_a = t_{aa}$ is the generalized occupation number for orbital a. The spin-angular coefficients t_{ab} and v^k_{abcd} appearing in (117) are evaluated using the same methods as for DHF [112, 113].

As in the nonrelativistic MCHF approach, it is possible to derive the MCDHF equations from the usual variational argument by varying both the large and small component:

$$w_a \begin{bmatrix} V_a(r) & -c\left(\frac{d}{dr}-\frac{\kappa_a}{r}\right) \\ c\left(\frac{d}{dr}+\frac{\kappa_a}{r}\right) & V_a(r)-2c^2 \end{bmatrix} \begin{bmatrix} P_a(r) \\ Q_a(r) \end{bmatrix} = \sum_b \varepsilon_{ab} \begin{bmatrix} P_b(r) \\ Q_b(r) \end{bmatrix} \tag{119}$$

Here $V(r) = (V_{nuc}(r) + Y(a;r) + \bar{X}(a;r)$ is the nuclear and direct potential, $\bar{X}(a;r)$ contain the contributions from all other Slater integrals and $V_{nuc}(r) = -Z/r$ in the case of a point nucleus. In each κ-space, Lagrange related energy parameters $\epsilon_{ab} = \epsilon_{n_an_b}$ are introduced to impose the orthonormality constraints (83) in the variational process. The method of solution for both the expansion coefficients and the radial functions are similar to those for the MCHF equations. The main difference

Compiled on 2016/01/23 at 13:08:13

is in the solution of the differential equations since the Dirac equations are a pair of first-order differential equations.

An interesting case for relativistic theory is that of the helium-like ground state for high-Z ions discussed in the MCHF section 4.2. A concern is the presence of negative energy states in an approximate wave function. Indelicato and Desclaux [137] claimed their convergence problems for natural orbital expansions, when orbitals with $n > 4$ were present, were due to the absence of projection operators. Among the $n = 4$ orbitals, only $4s$ converged. In a subsequent paper, Indelicato [138] introduced projection operators into an MCDHF calculation and claimed these were essential for a solution. But the difficulty could also have been due to numerical problems. With the GRASP92 [139] code, MCDHF results [140] were obtained for both U^{+90} and Ho^{+65} for He-like expansions up to $n = 6$ in good agreement with Indelicato's results including projection operators. The numerical problems can be understood already from the simple expansion over the $\{1s^2, 4f^2\}\ ^1S$ basis, which, in jj-coupling becomes $\{1s^2, 4f_+^2, 4f_-^2\}\ J = 0$. As Z increases, ultimately the contribution to the energy from $4f^2$ will be below the numerical accuracy of the solution of the equation for the $1s$ spinor. SCF iterations then are no longer meaningful unless the $1s$ is fixed and a perturbative method is applied.

In this review we have expressed the MCDHF equations in a manner that includes the generalized occupation number so that the matrix of Lagrange multipliers is symmetric. Correlation orbitals may have extremely low occupation number such as $t_{aa} = 10^{-6}$. In the present form division by small numbers is avoided and as $t_{aa} \to 0$, $\varepsilon_{aa} \to 0$. In the previous definition, the diagonal energy was proportional to ε_{aa}/t_{aa}, a ratio that approaches ∞ as $t_{aa} \to 0$ and would be of concern if the parameter were related to a binding energy. A derivation of the diagonal energy parameter for $\varepsilon_{4f_+4f_+}$ (or $\varepsilon_{4f_-4f_-}$) without the introduction of diagonal Lagrange multipliers has been published [141, 142] where it is shown that large Lagrange multipliers in the earlier definition implied that the $4f_+^2$ or $4f_-^2$ CSF was high in the positive energy continuum, as found in the earlier MCHF study. The one-electron energies of the $4f_-$ and $4f_+$ are shown as a function of Z in [142].

4.5. Brillouin's theorem, Breit, and QED corrections

The variational method can be applied to the $\mathcal{H}_{DCB}$ (19) with the consequence that Brillouin's theorem would be satisfied for selected excitations but at the cost of considerable computational effort. As in the case of the MCHF method (see Table 2) Brillouin's theorem alone is not sufficient for accuracy. Thus, this option has not been implemented in GRASP2K. Instead, larger expansions are used that allow for a systematic calculation.

4.5.1. Breit and QED corrections In the GRASP2K code, Breit and QED corrections are computed using the MCDHF orbitals from a calculation using the H_{DC} Hamiltonian and then applying the CI method with a Hamitonian that includes the desired corrections. Generally, the most important correction is the Breit correction with the Dirac-Coulomb-Breit Hamiltonian (19). In the GRASP2K code, by default, all corrections are included in the matrix elements for the Hamiltonian, such as $\mathcal{H}_{DCB+QED}$ (23). Thus they are not perturbative corrections and affect the wave function. When correlation orbitals with small generalized occupation numbers are

Compiled on 2016/01/23 at 13:08:13

Table 4. Comparison of total energies (in E_h) of the U^{+90} ground state for reduced and CAS expansions from CI calculations for different Hamiltonians when radial functions are computed for the reduced expansion.

Hamiltonian	Reduce	CAS	Diff.
DC	-9637.3780508	-9637.3780509	0.0000000
DCB	-9625.5384609	-9625.5959163	-0.0674554
DCB+VP	-9632.4011947	-9632.4491848	-0.0479901
DCB+VP+SE	-9606.0571813	-9606.1052038	-0.0480225
DCB+VP+SE*	-9606.0571795	-9606.1052020	-0.0480225

* Computed perturbatively

present, the correction to some individual matrix elements may become large. Then they could also be computed perturbatively, thereby not affecting the wave function.

The first QED correction, the self-energy contribution $\mathcal{H}_{SE}$, is applied to the diagonal energies as

$$\langle \Phi(\gamma_\alpha J)|\mathcal{H}_{SE}|\Phi(\gamma_\alpha J)\rangle \;=\; \sum_{a=1}^{n_w} w_a \; E_{SE}\,(a)\,, \tag{120}$$

where n_w is the number of subshells in the CSF, w_a is the number of electrons in subshell a in CSF, $E_{SE}\,(a)$ is the one-electron self-energy of an electron in subshell a. The way of estimating $E_{SE}\,(a)$ differs from one approach to another [143, 144].

The second QED correction included in GRASP2K is the vacuum polarization correction, applied to all matrix elements,

$$\langle \Phi(\gamma_\alpha J)|\mathcal{H}_{VP}|\Phi(\gamma_\beta J)\rangle \;=\; \langle \Phi(\gamma_\alpha J)|\sum_{i=1}^{N} V_{\rm Uehl}(r_i)|\Phi(\gamma_\beta J)\rangle, \tag{121}$$

where $V_{\rm Uehl}(r_i)$ also includes vacuum polarization potential terms of both second- and fourth-order in QED perturbation theory.

4.5.2. Consequence of changing the Hamiltonian As mentioned earlier, in GRASP2K the Breit and QED corrections are included in a CI calculation after the variational method has been used to determine radial functions. When expansions are compared with orbitals optimized for the $\mathcal{H}_{DCB}$, the CI mixing may be larger because of Brillouin's theorem not being satisfied although energy may be comparable. It should be remembered that the natural orbitals of a reduced form are optimized for a specific Hamiltonian. When the Hamiltonian changes the wave functions no longer satisfy Brillouin's theorem for the new Hamiltonian. In such cases, a full expansion may be needed for an accurate wave function. This can be seen from the following Table 4.5.2 where the difference in energy of the natural and CAS expansions for an $n = 3$ orbital set is shown for U^{+90}. For this highly charged ion, the difference is significant, although for the neutral He atom, the differences were negligible to the digits displayed.

4.5.3. Non-relativistic MCHF orbitals with a relativistic Hamiltonian A complementary low-order relativistic approach, also based on CI, consists of diagonalizing the Dirac-Coulomb-Breit Hamiltonian (19) interaction matrix to get a relativistic ASF representation (115) in a jj-CSF basis (52) built on Dirac spinors (10) whose large

Compiled on 2016/01/23 at 13:08:13

and small radial components are calculated from non-relativistic MCHF radial functions, using the Pauli approximation (24) [145, 64, 62]

$$P_{n\kappa}(r) = P_{nl}^{MCHF}(r) ,$$
$$Q_{n\kappa}(r) \simeq \frac{\alpha}{2}\left(\frac{d}{dr} + \frac{\kappa}{r}\right) P_{nl}^{MCHF}(r) . \quad (122)$$

These orbitals are then orthonormalized. This method, based on the use of a relativistic configuration interaction approach in the Pauli approximation, labelled RCI-P, provides an interesting way of checking the reliability of independent MCHF-BP calculations [142, 146].

4.5.4. Extended MCDHF methods Just as for the MCHF method the MCDHF method can be extended to simultaneously determine wave functions for many states. Again, the variational principle is applied to a weighted linear combination of functionals of the individual states and the energies and expansions coefficients are obtained as the corresponding eigenvalues and eigenvectors of the Hamiltonian matrix for the given symmetry [147]. Normally, wave functions for fine structure states of a given term are determined together. When determining wave functions for many states (up to a few hundred), calculations are often done by parity, meaning wave functions for all even states are determined in one calculation and wave functions for all odd states are determined in another [148, 149].

4.6. Eigenvector representation and jj to LSJ coupling transformations

The Breit-Pauli and MCDHF methods are both relativistic methods that clearly differ in a number of significant ways. One of these is the order of the coupling of the orbital quantum numbers. A Breit-Pauli calculation uses LSJ-coupling and in which radial functions of the orbitals depend only on nl-quantum numbers. As in all expansions where the basis CSFs form an orthonormal set, the square of the expansion coefficient represents the fraction of the composition of wave function accounted for by the given CSF. This information is used to determine the classification of the state. When relativistic effects are small, a specific LS value will account for most of the wave function composition and ideally is a single CSF. In the Atomic Spectra Database (ASD) at the National Institute of Standards and Technology (NIST) the designation of a level is usually associated with the CSF with the largest composition.

For the above reasons, it is often convenient to express results from an MCDHF calculation performed in jj-coupling in terms of LSJ notation. The JJ2LSJ code in GRASP2K does this by applying a unitary transformation to the MCDHF CSF basis set which preserves orthonormality. The unitary transformation selected is the coupling transformation that changes the order of coupling from jj to LSJ, a transformation that does not involve the radial factor, only the spin-angular factor.

As illustrated in section 3.2.1 for the $3d^4$ configuration, each nonrelativistic nl-orbital (except for ns) has associated with it two relativistic orbitals $l_\pm \equiv j = l \pm 1/2$. In the transformation of the spin-angular factor $|l^w \alpha LS\rangle$ into a jj-coupled angular basis, two subshell states, one with $l_- \equiv j = l - 1/2$ and another one with $l_+ \equiv j = l + 1/2$ may both occur in the expansion. This shell-splitting

$$|l^w \alpha \nu LS\rangle \longrightarrow \left(|l_-^{w_1}\ \nu_1 J_1\rangle,\ \ |l_+^{w_2}\ \nu_2 J_2\rangle\right) , \quad (123)$$

obviously conserves the number of electrons, provided ($w = w_1 + w_2$), with $w_1(\max) = 2l$ and $w_2(\max) = 2(l+1)$.

Compiled on 2016/01/23 at 13:08:13

Making use of this notation, the transformation between the subshell states in LSJ- and jj-coupling can be written as

$$|l^w \alpha\nu LSJ\rangle = \sum_{\nu_1 J_1 \nu_2 J_2 w_1} |(l_-^{w_1}\nu_1 J_1,\ l_+^{(w-w_1)}\nu_2 J_2)\ J\rangle\langle(l_-^{w_1}\nu_1 J_1,\ l_+^{(w-w_1)}\nu_2 J_2)\ J|l^w \alpha\nu LSJ\rangle, \quad (124)$$

$$|(l_-^{w_1}\nu_1 J_1,\ l_+^{(w-w_1)}\nu_2 J_2)\ J\rangle = \sum_{\alpha\nu LS} |l^w \alpha\nu LSJ\rangle\langle l^w \alpha\nu LSJ|l(l_-^{w_1}\nu_1 J_1,\ l_+^{(w-w_1)}\nu_2 J_2)\ J\rangle, \quad (125)$$

which, in both cases, includes a summation over all the quantum numbers (except of n, l_-, and l_+). Here, $|(l_-^{w_1}\nu_1 J_1,\ l_+^{w_2}\nu_2 J_2)\ J\rangle$ is a coupled angular state with well-defined total angular momentum J which is built from the corresponding jj-coupled subshell states with $j_1 = l_- = l - \frac{1}{2}$, $j_2 = l_+ = l + \frac{1}{2}$ and the total subshell angular momenta J_1 and J_2 , respectively.

An explicit expression for the coupling transformation coefficients

$$\langle(l_-^{w_1}\nu_1 J_1,\ l_+^{(w-w_1)}\nu_2 J_2)\ J|l^w \alpha\nu LSJ\rangle\ =\ \langle l^w \alpha\nu LSJ|(l_-^{w_1}\nu_1 J_1,\ l_+^{(w-w_1)}\nu_2 J_2)\ J\rangle \quad (126)$$

in (124) and (125) can be obtained only if we take the construction of the subshell states of w equivalent electrons from their corresponding *parent states* with $w-1$ electrons into account. In general, however, the *recursive* definition of the subshell states, out of their parent states, also leads to a recursive generation of the transformation matrices (126). These transformation coefficients can be chosen *real*: they occur very frequently as the *building blocks* in the transformation of all symmetry functions. The expressions and values of these configurations are published in [150].

5. Correlation models

5.1. Electron correlation

Hartree-Fock is an approximation to the exact solution of Schrödinger's equation. Neglected is the notion of "correlation in the motion of the electrons"; each electron is assumed to move independently in a field determined by the other electrons. For this reason, the error in the energy was defined by Löwdin in 1955 [151], to be the *correlation* energy, i.e.

$$E^{corr} = E^{exact} - E^{HF}. \quad (127)$$

In this definition, E^{exact} is the exact energy eigenvalue of Schrödinger's equation. In line with the definition we will refer to electron correlation as effects beyond the Hartree-Fock approximation. Electron correlation can be thought of as consisting of two parts; static correlation and dynamic correlation [152, 153].

5.2. Static electron correlation

The static correlation is a long-range re-arrangement of the electron charge distribution that arises from near degeneracies of the Hartree-Fock energies. Static correlation can be accounted for by including in the wave function a set of important CSFs that define the so called *multireference* (MR). Static correlation can also be interpreted in terms of Z- dependent perturbation theory and the CSFs in the MR are built from orbitals with the same principal quantum numbers as the ones that occupy the reference state and where we may think of orbitals with the same principal quantum numbers as being degenerate. In a more general setting we can say that the static correlation is

described by a set of CSFs that have large expansion coefficients and account for the major correlation effects.

5.3. Dynamic electron correlation

Dynamical correlation is a short-range effect that arises from the singularity of the $1/r_{ij}$ electron-electron interaction near points of coalescence where $r_{ij} = 0$ and has a cusp condition associate with it [51]. These are not isolated points, but include the entire region of space. The more likely regions are those where the probability of the finding a pair of electrons is the highest.

It has been shown that by extending expansions to include CSFs with higher l-quantum numbers, the accuracy of the wave function improves [154]. For the helium groundstate, a total energy accurate to seven (7) decimal places is estimated to require expansions up to $l = 100$ [84]. Wave function expansions in terms of CSFs built from central-field orbitals form a non-local basis that is non-zero over the region of space. If, instead, the CSF's are built from a B-spline basis, which is non-zero over only a "local" subregion, the contributions to expansions with higher l, have been shown to cluster around the $r_1 = r_2$ region [154, 56].

For $1sns$ triplet systems where the two electrons have the same spin, the wave function is zero at points where $r_1 = r_2$, including $r_{12} = 0$ due to the Pauli exclusion principle. Thus even at the HF level the two electrons are kept away from each other and the effects of dynamic electron correlation are fairly minor.

For many-electron systems the largest contributions to electron correlation come from pairs of electrons which occupy the same region in space. Thus there are large contributions from each doubly occupied orbital with smaller additions from orbital pairs that occupy different shells. Just as for the static correlation the dynamic correlation can be accounted for by expansions over CSFs and the effect should be to mimic the cusp behavior of the exact wave function at points of electron coalescence. Perturbative arguments are used to define classes of CSFs that are important in this regard and this is the topic of the next section.

5.4. Z-dependent perturbation theory

Let us introduce a new variable $\rho = Zr$, which in effect changes the unit of length. Then the Hamiltonian becomes

$$\mathcal{H} = Z^2 \left(\mathcal{H}^0 + Z^{-1} V \right), \tag{128}$$

where

$$\mathcal{H}^0 = \sum_{i=1}^{N} \left(-\frac{1}{2}\nabla_i^2 - \frac{1}{\rho_i} \right), \qquad V = \sum_{i>j}^{N} \frac{1}{\rho_{ij}}. \tag{129}$$

Schrödinger's equation now reads

$$\left(\mathcal{H}^0 + Z^{-1} V \right) \Psi = \left(Z^{-2} E \right) \Psi. \tag{130}$$

In this form, the $1/Z$ appears as the natural perturbation parameter. If we assume

$$\Psi = \Psi^0 + Z^{-1}\Psi^1 + Z^{-2}\Psi^2 + \cdots \tag{131}$$

in the ρ unit of length, and

$$E = Z^2 \left(E^0 + Z^{-1}E^1 + Z^{-2}E^2 + Z^{-3}E^3 + \cdots \right) \tag{132}$$

Compiled on 2016/01/23 at 13:08:13

we may insert these expansions in (130) to obtain equations for Ψ^k and E^k;

$$\begin{aligned}(\mathcal{H}^0 - E^0)\Psi^0 &= 0\\ (\mathcal{H}^0 - E^0)\Psi^1 &= (E^1 - V)\Psi^0\\ (\mathcal{H}^0 - E^0)\Psi^2 &= (E^1 - V)\Psi^1 + E^2\Psi^0.\end{aligned} \tag{133}$$

The solutions of the first equation are products of hydrogenic orbitals.

Let $|\{nl\}\gamma LS\rangle$ be a configuration state function constructed from products of hydrogenic orbitals. Here $\{nl\} = \{n_1 l_1, n_2 l_2, \ldots, n_N l_N\}$ is the set of N principal and orbital quantum numbers that define the configuration (35) and γ denotes the complete set of the coupling tree quantum numbers specifying unambiguously the considered configuration state (see (46)). Then

$$\mathcal{H}^0|\{nl\}\gamma LS\rangle = E^0|\{nl\}\gamma LS\rangle \tag{134}$$

with E^0 being the sum of the hydrogenic energies

$$E^0 = \sum_{i=1}^{N}\left(-\frac{1}{2n_i^2}\right). \tag{135}$$

Since E^0 is independent of the orbital quantum numbers, it is now clear that different configurations may lead to the same E^0; that is, E^0 is degenerate. According to first-order perturbation theory for degenerate states [97, 155], Ψ^0 is a linear combination of the degenerate configuration state functions $|\{nl'\}\gamma' LS\rangle$; the coefficients are components of an eigenvector of the interaction matrix, $\langle\{nl'\}\gamma' LS|V|\{nl\}\gamma LS\rangle$ and E^1 is the corresponding eigenvalue. Then

$$\Psi^0 = \sum_{l'\gamma'} c_{l'\gamma'}\ |\{nl'\}\gamma' LS\rangle. \tag{136}$$

But only configurations with the same parity interact and so the linear combination is over all CSFs with the same set of principal quantum numbers and the same parity. This set of CSFs is referred to as the *complex* by Layzer *et al.* [156].

The first-order correction Ψ^1 is a solution of (133) orthogonal to Ψ^0. It can be expanded as a linear combination of normalized intermediate configuration state functions $|\gamma_v LS\rangle$ belonging to $\mathcal{H}^0$, but outside the complex. Then

$$\Psi^1 = \sum_v \frac{|\gamma_v LS\rangle\langle\gamma_v LS|V|\Psi^0\rangle}{E^0 - E_{\gamma_v LS}} \tag{137}$$

where $E_{\gamma_v LS} = \langle\gamma_v LS|\mathcal{H}^0|\gamma_v LS\rangle$. Substituting equation (136) into (137) and interchanging the orders of summation, we find

$$\Psi^1 = \sum_{l'\gamma'} c_{l'\gamma'} \sum_v \frac{|\gamma_v LS\rangle\langle\gamma_v LS|V|\{nl'\}\gamma' LS\rangle}{E^0 - E_{\gamma_v LS}}. \tag{138}$$

In other words, the mixing coefficient, $c_{l'\gamma'}$, is a weight factor in the sum over intermediate configuration state functions $|\gamma_v LS\rangle$ interacting (having non-zero matrix elements) with configuration state functions in the complex.

5.5. Classification of correlation effects

The zero-order wave function Ψ^0 is obtained as a linear combination of CSFs in the complex. It describes the many-electron system in a general way and accounts for the major part of the long-range static electron correlation. The first-order correction Ψ^1 is a linear combination of CSFs that interact with the CSFs in the complex and it accounts for additional long-range electron correlation and the major part of the short range dynamic correlation. Assume for simplicity that there is only one configuration state function $|\{nl\}\gamma LS\rangle$ in the complex. The CSFs interacting with $|\{nl\}\gamma LS\rangle$ are of two types: those that differ by a single electron (single substitution S) and those that differ by two electrons (double substitution D). The former can be further subdivided into

(i) Those that differ from $|\{nl\}\gamma LS\rangle$ by one principal quantum number but retain the same spin and orbital angular coupling. These configuration states are part of *radial correlation*.

(ii) Those that differ by one principal quantum number and also differ in their coupling. Often the only change is the coupling of the spins, in which case the configuration states are part of *spin-polarization*.

(iii) Those that differ in the angular momentum of exactly one electron and are accompanied by a change in orbital angular coupling of the configuration state and possibly also the spin coupling. The latter represent *orbital polarization*.

The sums over CSFs that differ in two electrons can also be classified. Let $\{a, b, c, ..\}$ be occupied orbitals in $\{nl\}\gamma LS$ and $\{v, v', ..\}$ be orbitals in a so called active set. Then the double replacement $ab \rightarrow vv'$ generates CSFs in the expansion for Ψ^1. The function defined by CSFs from all double replacements from ab is called a pair-correlation function (PCF) and it corrects for the cusp in the wave function associated with this electron pair. The PCFs from all electron pairs correct for the main part of the dynamic correlation. There is another and more general classification that takes into account if the orbital replacements are from valence or core orbitals:

(i) If ab are orbitals for outer electrons the replacement represents outer or *valence correlation*.

(ii) If a is core orbital but b is an outer orbital, the effect represents the polarization of the core and is referred to as *core-valence correlation*.

(iii) If both orbitals are from the core, the replacement represents *core-core correlation*.

5.6. CSF expansions for energy

Z-dependent perturbation theory is not appropriate for practical calculations, but it is a very useful guide for how the initial HF approximation can be improved in MCHF or CI calculations in order to capture most of the correlation energy. The zero-order wave function Ψ^0 accounting for the major part of the static correlation is an expansion over CSFs with large interactions with the CSF of interest, either those that are nearly degenerate or those with a large interaction matrix element (see section 4.1.1). These CSFs are said to define the *multireference* (MR) set. Further, to account for dynamic correlation, the wave function Ψ should include, in addition to the CSFs in the MR set, CSFs generated by SD replacements of orbitals in the CSFs of the MR with orbitals in an active set (AS). The included CSFs should interact with one or more CSFs in the MR.

Compiled on 2016/01/23 at 13:08:13

As an example we look at $1s^22s^2\ ^1S$. For infinite Z, $1s^22s^2\ ^1S$ is degenerate with $1s^22p^2\ ^1S$ and degenerate perturbation theory needs to be applied. Here, for finite Z, the zero-order wave function is an expansion over the two CSFs $\{|1s^22s^2\ ^1S\rangle,\ |1s^22p^2\ ^1S\rangle\}$ that define the MR set. For Be I we have

$$\Psi^0 = 0.9500344|1s^22s^2\ ^1S\rangle + 0.3121452|1s^22p^2\ ^1S\rangle \tag{139}$$

and we see that both the CSFs in the MR set have large expansion coefficients (generally greater than a few per cent of the wave function). Valence correlation is accounted for by considering CSFs obtained from $2s2s \rightarrow nln'l'$ replacements from the first CSF in the MR or, alternatively by $2p2p \rightarrow nln'l'$ replacements from the second CSF in the MR. Core-valence correlation is accounted for by considering CSFs obtained from $1s2s \rightarrow nln'l'$ and $1s2p \rightarrow nln'l'$ replacements from, respectively, the first and second CSF in the MR. Core correlation in the $n = 1$ shell accounted for by considering CSFs obtained from $1s1s \rightarrow nln'l'$ replacements from both CSFs in the MR. All the generated CSFs should interact with the CSFs in the MR. Included in the general expansions above are also the CSFs obtained by single replacements, although there is no clear classification in valence, core-valence or core correlation effects.

The generation of the CSF expansions is a very important step in atomic structure calculations. In the ATSP2K and GRASP2K program packages there are flexible program modules for generating CSF expansions based on rules for orbital replacements from an MR to active sets of orbitals [157, 158].

5.7. Correlation and spatial location of orbitals

In the MCHF and MCDHF methods the location and shape of the correlation orbitals depend on the energy functional or CSFs expansion used to derive the MCHF or MCDHF equations [48, 159]. To illustrate this we again consider the ground state of Be I. Figure 2 displays orbitals from MCHF calculations based on CSFs expansions describing valence-, core-valence and core correlation, respectively. One clearly sees the contraction of the correlation orbitals when going from a valence to a core correlation calculation.

Orbitals in the valence region are ill suited to describe correlation in the core region and vice versa. Since calculations due to orthogonality constraints are based on one orbital set, this must often be large to saturate all correlation effects. This is especially true for large systems with many subshells. To overcome these problems the Partitioned Correlation Function Interaction (PCFI) method has been developed [159, 160]. The PCFI method uses a biorthonormal transformation method [161] to relax the orthogonality constraint of the orbitals and correlation effects can be described by several non-orthogonal sets of correlation orbitals, each set being optimally localized for the considered correlation effect. The PCFI method captures correlation effects more efficiently than the ordinary MCHF and MCDHF methods [50].

5.8. CSF expansions for energy differences

Often we are interested in determining *energy separations* between different levels. In these cases we may, in the first approximation, define closed inner subshells as *inactive* and consider correlation only between the outer valence electrons. The rationale for this is that the correlation energy in the core, although large in an absolute sense, to a great extent cancels when computing energy level differences or the energy relative

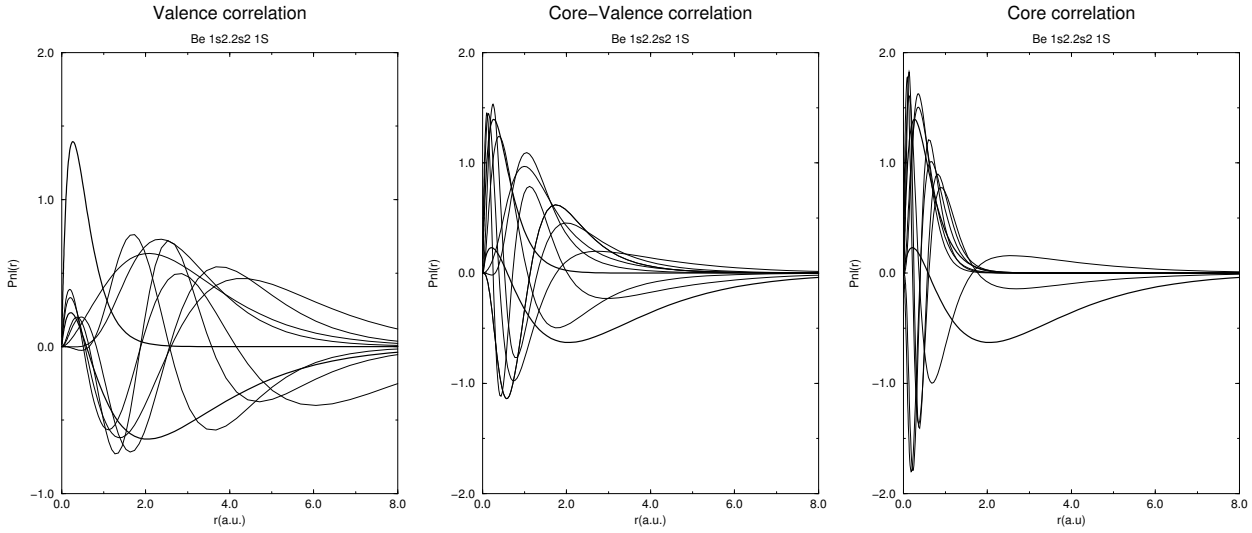

Figure 2. Contraction of the correlation orbitals from valence, core-valence and core-core correlation MCHF calculations of Be $1s^2 2s^2\ ^1S$. The two thick lines correspond to the spectroscopic $1s$ (no node) and $2s$ (one node) orbitals. Other lines represents the radial distributions of the correlation orbitals of the $n = 4$ active set.

to the ground state. However, the presence of outer valence electrons polarizes the core. The polarization, or core-valence correlation, is represented by CSFs obtained by orbital replacements $ab \rightarrow vv'$ from the CSFs of the multireference where a and b, respectively, are core and valence orbitals.Question: what is the correct terminology: core-polarization is just one excitation from the core? I tend to talk about core-polarization and core-valence roughly meaning the same thing but I guess it is not. How to write this correctly. Should one say that the outer electron affects the core and then just not introduce core-polarization? (Core-polarization in Ca I and Ca II [162]) The core-valence correlation reduces the energy and increases the binding of the valence electrons to the core. In case of a single electron the increase in the binding is reflected in a *contraction* of the orbital which has a large effect on other computed properties.

Generally, energy separations are much improved if also core-valence correlation is included. For larger atomic systems it is not always clear which subshells should be inactive and which should be part of the active core for which core-valence effects are to be considered. For each new system this needs to be systematically investigated. Somewhat counter intuitive there are several examples where core-valence correlation effects are larger for more inner subshells than for more outer subshells [18]. A good starting point point analyzing the situation is to plot the radial part of the core and valence orbital and look at the overlap between the different orbitals. If the overlap is larger core-valence effects are likely to be important.

To illustrate the discussion above we look at the separation between $1s^2 2s^2 2p^6 3s\ ^2S$ and $1s^2 2s^2 2p^6 3p\ ^2P^o$ in Na I. We systematically include CSFs obtained

Table 5. Energies (in E_h) for $3s\ ^2S$ and $3p\ ^2P^o$ of Na I as more correlation types of CSFs are added to the wave function expansion.

Corr.	$E(^2S)$	$E(^2P^o)$	ΔE
HF	−161.858580	−161.786286	0.072293
$2pv$	−161.866176	−161.788935	0.077241
$2p2p$	−162.076793	−161.999811	0.076981
$2sv$	−162.077481	−162.000103	0.077378
$2s2p$	−162.158012	−162.081373	0.076639
$2s2s$	−162.169542	−162.093022	0.076520
$1sv$	−162.169625	−162.093066	0.076558
$1s2p$	−162.193467	−162.117022	0.076445
$1s2s$	−162.199039	−162.122580	0.076460
$1s1s$	−162.238215	−162.161813	0.076402

from

$$2pv \rightarrow nln'l', \quad 2p2p \rightarrow nln'l', \quad 2sv \rightarrow nln'l',$$
$$2s2p \rightarrow nln'l', \quad 2s2s \rightarrow nln'l', \quad 1sv \rightarrow nln'l',$$
$$1s2p \rightarrow nln'l', \quad 1s2s \rightarrow nln'l', \quad 1s1s \rightarrow nln'l', \tag{140}$$

replacements from the $|1s^22s^22p^63s\ ^2S\rangle$ and $|1s^22s^22p^63p\ ^2P^o\rangle$ reference CSFs to an active set that was extended to principal quantum numbers $n = 9$ and orbital quantum numbers $l = 5$ leading to energy contributions that are reasonably well converged with respect to the orbital set. Here v denote the $3s$ or $3p$ valence orbital. The accumulated contributions to the total energy of the two states as well to the energy difference is from the CSFs obtained from the replacements are displayed in Table 5.

From the table we see that CSFs obtained by orbital replacements $2pv \rightarrow nln'l'$, accounting for the core-valence correlation with $2p$, have a relatively small influence on the total energies. The CSFs are however *very* important for the energy differences. CSFs obtained by orbital replacements $2p2p \rightarrow nln'l'$ account by far for most of the correlation energies in the two states. These contributions largely cancel and the change in the energy difference is rather small, of the same order as the effect of the $2sv \rightarrow nln'l'$ replacements the describe the core-valence electron correlation with $2s$. Also the correlation between $2s$ and $2p$ described by the $2sv \rightarrow nln'l'$ replacements are important for both the total energies and the energy differences.

5.9. Capturing higher-order correlation effects

Z-dependent perturbation theory defines the structure of the zero-order wave function and the first-order correction. The structure of higher-order corrections for energies, as well as other properties, can be derived in a similar way. For energies, higher-order corrections are captured by including CSFs that interact with the CSFs in the zero- and first-order wave function. In practice this is the same as including some of the CSFs that can be generated by single, double, triple, and quadruple (SDTQ) orbital replacements $abcd \rightarrow vv'v''v'''$ from the CSFs of the multireference. The number of CSFs increases very rapidly with the increasing number of orbitals in the active set and thus general SDTQ or SDT orbital replacements are feasible only for

Compiled on 2016/01/23 at 13:08:13

few-electron systems [163, 164]. A way to include the most important higher-order correlation effects is to increase the MR by adding CSFs for a certain portion of the wave function composition [165, 166]. The overall accuracy of the wave function increases as MR accounts for a larger portion of the wave function. In fact, if MR represents the portion p of the total wave function and $E - E^{\rm MR}$ the amount by which the SD excitations have lowered the energy then an estimate of the error in the energy is $(E - E^{\rm MR})(1 - p)/p$ [167, 168].

5.10. Valence and core-valence correlation in lanthanides

In a relatively simple system, it may be sufficient to have a balanced SD process applied similarly to the odd and even parity states and a common fixed core. But complex, heavy atoms require more care. Consider a ground state calculation for the odd $4f5d6s^2$ configuration of Ce I, a lanthanide element, with a nearby interacting $4f5d^26s$ configuration. The lowest even parity configuration is the $4f^26s^2$ configuration fairly high in the spectrum. Calculations for this spectrum have not been investigated, to our knowledge, but, would raise a number of issues.

It is not obvious what the core should be. Configurations are specified by listing open sub-shells in order of energy of the electrons or possibly a closed, outer s^2 sub-shell. In the case of Ce I, inner closed sub-shells are $1s^22s^22p^63s^23p^63d^{10}4s^24p^64d^{10}5s^25p^6$. Notice that both the $n = 4$ shell and the $n = 5$ shells are unfilled as well as the $n = 6$ shell. The notation implies the occupied subshells, $4f, 5d, 6s$ are outside the core but the Fig. 3 shows that the mean radius of the $4f$ orbital is close to that of $4d$ and that, from the point of view of "correlation in the motion of the electrons"there may well be more $4d - 4f$ interaction than, say $5p - 4f$. It is possible that $4f$ should be considered part of the core, so that its main role is to define the screening of the outer orbitals. It would imply that $4f^26s6p$, for example, should be considered as a system with a larger core, with its own set of outer correlation orbitals, non-orthogonal to those of $4f5d6s^2$.

For the lanthanides, it is not clear how the concept of core and valence electrons can be applied. For the ground configuration of Ce I, the complex theory would require $5s, 5p, 5d, 6s$ to be occupied valence orbitals and possibly also other orbitals depending on the strength of interactions between CSFs in the $\{1\}^2\{2\}^8\{3\}^{18}\{4\}^{19}\{5\}^9\{6\}^2$ complex. We could make the assumption that correlation within the $n = 4$ shell is the same for all levels and cancels in an energy difference but could be included as part of core-core correlation. This leads so to the concept of three types of orbitals:

(i) An inactive core – $1s, 2s, 2p, 3s, 3p, 3d$

(ii) An active core – $4s, 4p, 4d, 4f$

(iii) Valence orbitals – $5s, 5p, 5d, 6s$

In addition to difficulties in defining the core, calculations for the lanthanides suffer from the fact that the number of CSFs generated by SD substitutions from a MR rapidly grow unmanageably large. Configurations, however, can be ranked according to their interaction strength [169]. Retaining only the most important configurations reduces the number of CSFs, but still calculations strain computational resources and only a few correlation studies have been reported. Examples include the $4f^2$ configuration of Pr IV [170].
(We might need to cite Safronova *et al.* [171]. We should read the paper in any case.)

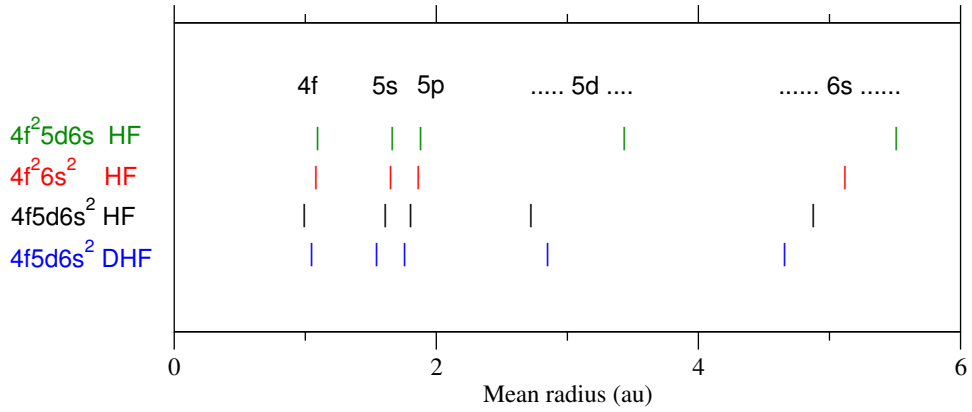

Figure 3. HF and DHF radii of orbitals of some configurations of Ce I

6. Estimating uncertainties

To estimate the uncertainties in computed atomic parameters the list of CSFs should be enlarged in a systematic way. This can be done in a number of ways and in practice there is always a balance between the available computational resources and desired accuracy. The following steps can be followed:

(i) increase the orbital set systematically and monitor the convergence of the desired property

(ii) expand the MR so SD substitutions are applied to a larger portion of the wave function

(iii) for a given MR, monitor the convergence for different subsets of the MR

(iv) relax any constraint (such as an inactive core) in the correlation model

6.1. A systematic approach

Lithium has been a much studied system due to the possibility of systematically exploring and understanding different correlation effects and convergence properties of the variational solution. For lithium there also are a number of highly accurate Hylleraas variational calculation for comparison. The non-relativistic total energies for the latter calculations are essentially exact. Tong *et al.* [45] studied the convergence of the total energy for $1s^2 2s\ ^2S$ in Li I for nl-expansions, similar to partial wave expansions. The generation of the CSFs can be described by

For $l_1, l_2, l_3 \leq 0, 1, \ldots, L$
  For $n_1, n_2, n_3 \leq 1, 2, \ldots, N$
    Include CSFs of the form $|n_1 l_1 n_2 l_2 n_3 l_3\ ^2S\rangle$

where L and N are upper limits on l_1, l_2, l_3 and n_1, n_2, n_3 respectively. The result is displayed in Table 6. The column headed n denotes the largest n of the current l column and for $l > 0$, the calculation includes all the orbitals of the previous columns. Thus the calculations for $n = 2,\ l = 1$ includes all CSFs that can be generated by SDT replacements of orbitals in the $1s^2 2s$ reference with orbitals in the active set $\{1s, 2s, \ldots, 13s, 2p\}$. The row denoted ∞ contains extrapolated values for each l. The

Compiled on 2016/01/23 at 13:08:13

Table 6. Total energies (in E_h) from nl-expansions for $1s^2 2s\ ^2S$ in Li I as a function of the maximum values of n and l (from Ref. [45])

n	$l=0$	$l=1$	$l=2$	$l=3$	$l=4$
2	-7.432 726 93	-7.469 941 45			
3	-7.447 567 56	-7.471 977 24	-7.476 040 54		
4	-7.448 476 36	-7.473 217 44	-7.476 483 19	-7.477 263 40	
5	-7.448 610 63	-7.473 628 47	-7.476 610 99	-7.477 406 14	-7.477 667 73
6	-7.432 644 19	-7.473 765 36	-7.476 695 98	-7.477 455 71	-7.477 725 20
7	-7.447 656 86	-7.473 809 59	-7.476 734 50	-7.477 477 01	-7.477 748 59
8	-7.448 662 54	-7.473 824 87	-7.476 751 83	-7.477 491 03	-7.477 759 33
9	-7.448 664 96	-7.473 830 96	-7.476 760 26	-7.477 498 88	-7.477 764 96
10	-7.432 666 06	-7.473 833 71	-7.476 764 37	-7.477 503 03	-7.477 768 82
11	-7.447 666 61	-7.473 835 09	-7.476 766 47	-7.477 505 39	-7.477 771 22
12	-7.448 666 90	-7.473 835 86	-7.476 767 61	-7.477 506 78	-7.477 772 64
13	-7.448 667 06	-7.473 836 26	-7.476 768 26	-7.477 507 61	-7.477 773 50
14		-7.473 836 52	-7.476 768 66	-7.477 508 12	-7.477 774 08
∞	-7.448 667 26	-7.473 836 90	-7.476 769 24	-7.477 508 95	-7.477 775 17
δ_l	-0.000 000 20	-0.000 000 38	-0.000 000 58	-0.000 000 83	-0.000 001 09
$+\delta$	-7.448 667 26	-7.473 837 10	-7.476 769 82	-7.477 510 11	-7.477 777 16

extrapolated values can be obtained using the fact that ratio of the energy differences $r_n = \Delta E_n / \Delta E_{n-1}$ where $\Delta E_n = E_n - E_{n-1}$ is almost constant and in the range 0.5 – 0.6. This leads to a geometric series for the correction which sums up to

$$\Delta E_n \left(\frac{r_n}{1 - r_n} \right) \tag{141}$$

With r_n in the above range the correction is similar to the last corrections ΔE_n to the energy. The row denoted δ_l shows the correction between the extrapolated values and the last energy computed for the partial wave. When starting the calculations for a new partial wave l the correction δ_{l-1} from the previous wave needs to be added (for details see the original article). The table shows that the energy converges well within a given partial wave. However, to obtain the total energy the contributions from the high-l partial waves must be estimated. Assuming a similar asymptotic behavior with respect to l as was for two-electron systems $\Delta E^l = E^l - E^{l-1}$, where E^l is the limit for the l partial wave, is fitted to an expression of the form

$$a_0 \left(l + \frac{1}{2} \right)^{-4} + a_1 \left(l + \frac{1}{2} \right)^{-5} + a_2 \left(l + \frac{1}{2} \right)^{-6} \tag{142}$$

The remainder is obtained by summing the above expression over l. This gives the final non-relativistic total energy for $1s^2 2s\ ^2S$ in Li I

$$E_{nr} = -7.478\ 059\ 6\ \mathrm{E}_h \tag{143}$$

Similar detailed and systematic convergence studies of energies have been done for other Li-like systems [49] as well as for Be- and B-like systems [47, 48, 159, 50], adding to our understanding of correlation effects and how they can be accounted for in multiconfiguration methods.

Compiled on 2016/01/23 at 13:08:13

7. Concluding Remarks

In this review we have presented the basic theory for generating multiconfiguration wave functions using variational methods that optimize an energy expression in both nonrelativistic and relativistic frameworks. Conceptually, such wave functions could be sufficiently accurate for predicting any atomic property. But the many-body aspects often limit the accuracy of a calculation. Predictions can be improved with expansions that take into account the atomic property under investigation.

Applications that have been extensively investigate are spectrum calculations for all levels up to a designated excited level, allowed and forbidden transitions [131, 136, 172, 173, 53], isotope shifts [174, 175, 176, 166, 177, 178], hyperfine structures [179, 146, 180, 181], nuclear effects on transition rates and spectra [25, 182], magnetic field-induced transitions [183, 184, 19], to name a few. The method described here are important for the calculation of target states for R-matrix calculations, BSR [185, 186] for non-relativistic and DBSR [187, 188] for relativistic versions, that describe collision, excitation, and scattering processes such as those needed for plasma diagnostics. Another review paper focusing on the applications is being considered.

8. References

[1] E. Schrödinger. An undulatory theory of the mechanics of atoms and molecules. *Phys. Rev.*, 28:1049–1070, Dec 1926.

[2] P.A.M. Dirac. The quantum theory of the electron. *Proc. R. Soc. Lond. A*, 117:610, 1928.

[3] P.A.M. Dirac. The quantum theory of the electron. part ii. *Proc. R. Soc. Lond. A*, 118:351, 1928.

[4] E.A. Hylleraas. ber den grundzustand des heliumatoms. *Zeitschrift fr Physik*, 48(7-8):469–494, 1928.

[5] E.A. Hylleraas. Neue berechnung der energie des heliums im grundzustande, sowie des tiefsten terms von ortho-helium. *Zeitschrift für Physik A Hadrons and Nuclei*, 54:347–366, 1929. 10.1007/BF01375457.

[6] D.R. Hartree. The calculation of atomic structures. *Rep. Prog. Phys.*, 11:113, 1946-1947.

[7] B. Edlén. Wavelength measurements in the vacuum ultra-violet. *Reports on Progress in Physics*, 26(1):181, 1963.

[8] B. Edlén. Atomic spectra. In S. Flgge, editor, *Spectroscopy I / Spektroskopie I*, volume 5 / 27 of *Encyclopedia of Physics / Handbuch der Physik*, pages 80–220. Springer Berlin Heidelberg, 1964.

[9] C.J. Joachain. High-intensity laser-atom interactions. *EPL (Europhysics Letters)*, 108(4):44001, 2014.

[10] C. Amole, M. D. Ashkezari, M. Baquero-Ruiz, W. Bertsche, E. Butler, A. Capra, C. L. Cesar, M. Charlton, S. Eriksson, J. Fajans, T. Friesen, M. C. Fujiwara, D. R. Gill, A. Gutierrez, J. S. Hangst, W. N. Hardy, M. E. Hayden, C. A. Isaac, S. Jonsell, L. Kurchaninov, A. Little, N. Madsen, J. T. K. McKenna, S. Menary, S. C. Napoli, P. Nolan, K. Olchanski, A. Olin, A. Povilus, P. Pusa, C. Ø. Rasmussen, F. Robicheaux, E. Sarid, D. M. Silveira, C. So, T. D. Tharp, R. I. Thompson, D. P. van der Werf, Z. Vendeiro, J. S. Wurtele, A. I. Zhmoginov, and A. E. Charman. An experimental limit on the charge of antihydrogen. *Nat Commun*, 5, 06 2014.

[11] P.J. Mohr, B.N. Taylor, and D.B. Newell. CODATA recommended values of the fundamental physical constants: 2010. *J. Phys. Chem. Ref. Data*, 41:043109, 2012.

[12] Z.-T. Lu, P. Mueller, G.W.F. Drake, W. Nörtershäuser, S.C. Pieper, and Z.-C. Yan. *Colloquium* : Laser probing of neutron-rich nuclei in light atoms. *Rev. Mod. Phys.*, 85:1383–1400, Oct 2013.

[13] V.A. Dzuba, V.V. Flambaum, and B. Roberts. Calculation of the parity-violating $5s$-$6s$ $e1$ amplitude in the rubidium atom. *Phys. Rev. A*, 86:062512, Dec 2012.

[14] J.C. Berengut and V.V. Flambaum. Manifestations of a spatial variation of fundamental constants in atomic and nuclear clocks, oklo, meteorites, and cosmological phenomena. *EPL (Europhysics Letters)*, 97(2):20006, 2012.

[15] N. Leefer, C.T.M. Weber, A. Cingöz, J.R. Torgerson, and D. Budker. New limits on variation of the fine-structure constant using atomic dysprosium. *Phys. Rev. Lett.*, 111:060801, Aug 2013.

[16] D.A. Gurnett and A. Bhattacharjee. *Introduction to Plasma Physics: With Space and Laboratory Applications*. Cambridge University Press, Edinburgh Gate, Harlow, England, 2005.

[17] P. Beiersdorfer. Highly charged ions in magnetic fusion plasmas: research opportunities and diagnostic necessities. *Journal of Physics B: Atomic, Molecular and Optical Physics*, 48(14):144017, 2015.

[18] J. Grumer, T. Brage, M. Andersson, J. Li, P. Jönsson, W. Li, Y. Yang, R. Hutton, and Y. Zou. Unexpected transitions induced by spin-dependent, hyperfine and external magnetic-field interactions. *Physica Scripta*, 89(11):114002, 2014.

[19] J. Li, T. Brage, P. Jönsson, and Y. Yang. Magnetic-field-dependent angular distributions and linear polarizations of emissions from the $2p^5 3s\ ^3P_2^o$ state in ne-like ions. *Phys. Rev. A*, 90:035404, Sep 2014.

[20] Y. Ralchenko. Online databases and computational tools for non-lte spectroscopy. *Physica Scripta*, 2009(T134):014025, 2009.

[21] A. Dasgupta, R.W. Clark, N.D. Ouart, and J.L. Giuliani. Cu spectroscopy from a z-pinch plasma. *Physica Scripta*, 89(11):114008, 2014.

[22] P. Jönsson, S.G. Johansson, and C. Froese Fischer. Accurate calculation of the isotope shift and hyperfine structure in the boron (B II) line at 1362 A. *Astrophysical Journal Letters*, 429:L45–L48, July 1994.

[23] S.R. Federman, D.L. Lambert, J.A. Cardelli, and Y. Sheffer. The boron isotope ratio in the

interstellar medium. *Nature*, 381(6585):764–766, 06 1996.
[24] L. Rebull, D. Duncan, S. Johansson, J. Thorburn, and B. Fields. Limits on the boron isotopic ratio in hd 76932. *The Astrophysical Journal*, 507(1):387, 1998.
[25] T. Brage, P.G. Judge, A. Aboussaïd, M. Godefroid, C. Froese Fischer, P. Jönsson, A. Ynnerman, and D. Leckrone. Hyperfine induced transitions as diagnostics of isotopic compositttion and densities of low-density plasmas. *Astrophys. J*, 500:507–521, 1998.
[26] S. Johansson, U. Litzén, H. Lundberg, and Z. Zhang. Experimental f-value and isotopic structure for the ni i line blended with [o i] at 6300 å. *The Astrophysical Journal Letters*, 584(2):L107, 2003.
[27] C. Sneden, J.E. Lawler, M.P. Wood, E.A. Den Hartog, and J.J. Cowan. Atomic data for stellar spectroscopy: recent successes and remaining needs. *Physica Scripta*, 89(11):114006, 2014.
[28] Editorial. Nailing fingerprints in the stars. *Nature*, 503:437, 2013.
[29] C. Froese Fischer and G. Gediminas. Multiconfiguration dirac-hartree-fock energy levels and transition probabilities for w xxxviii. *Phys. Rev. A*, 85:042501, Apr 2012.
[30] C. Froese Fischer. Evaluation and comparison of configuration interaction calculations for complex atoms. *atoms*, 2014.
[31] T.I. Madeira, P. Amorim, F. Parente, P. Indelicato, and J.P. Marques. On the interpretation of tungsten emission spectra in fusion devices. *Physica Scripta*, 2013(T156):014011, 2013.
[32] S. Morita, C.F. Dong, M. Goto, D. Kato, I. Murakami, H.A. Sakaue, M. Hasuo, F. Koike, N. Nakamura, T. Oishi, A. Sasaki, and E.H. Wang. A study of tungsten spectra using large helical device and compact electron beam ion trap in nifs. *AIP Conference Proceedings*, 1545(1):143–152, 2013.
[33] T. Pütterich, V. Jonauskas, R. Neu, R. Dux, and ASDEX Upgrade Team. The extreme ultraviolet emissions of w23+(4f5). *AIP Conference Proceedings*, 1545(1):132–142, 2013.
[34] GIANO spectrograph. GIANO is a near IR high resolution spectrograph mounted at the Nasmyth A focus of the TNG, Fundacin Galileo Galilei - INAF, Fundacin Canaria" (FGG).
[35] H.-U. Käufl, P. Ballester, P. Biereichel, B. Delabre, R. Donaldson, R. Dorn, E. Fedrigo, G. Finger, G. Fischer, F. Franza, D. Gojak, G. Huster, Y. Jung, J.-L. Lizon, L. Mehrgan, M. Meyer, A. Moorwood, J.-F. Pirard, J. Paufique, E. Pozna, R. Siebenmorgen, A. Silber, J. Stegmeier, and S. Wegerer. CRIRES: a high-resolution infrared spectrograph for ESO's VLT. In A. F. M. Moorwood and M. Iye, editors, *Ground-based Instrumentation for Astronomy*, volume 5492 of *Society of Photo-Optical Instrumentation Engineers (SPIE) Conference Series*, pages 1218–1227, September 2004.
[36] E.T. Young, E.E. Becklin, P.M. Marcum, T.L. Roellig, J.M. De Buizer, T.L. Herter, R. Gsten, E.W. Dunham, P. Temi, B.-G. Andersson, D. Backman, M. Burgdorf, L. J. Caroff, S.C. Casey, J.A. Davidson, E.F. Erickson, R.D. Gehrz, D.A. Harper, P.M. Harvey, L.A. Helton, S.D. Horner, C.D. Howard, R. Klein, A. Krabbe, I.S. McLean, A. W. Meyer, J.W. Miles, M.R. Morris, W.T. Reach, J. Rho, M.J. Richter, H.-P. Roeser, G. Sandell, R. Sankrit, M.L. Savage, E.C. Smith, R.Y. Shuping, W.D. Vacca, J.E. Vaillancourt, J. Wolf, and H. Zinnecker. Early science with sofia, the stratospheric observatory for infrared astronomy. *The Astrophysical Journal Letters*, 749(2):L17, 2012.
[37] P. Beiersdorfer. Spectroscopy with trapped highly charged ions. *Physica Scripta*, 2009(T134):014010, 2009.
[38] J.D. Gillaspy. Precision spectroscopy of trapped highly charged heavy elements: pushing the limits of theory and experiment. *Physica Scripta*, 89(11):114004, 2014.
[39] Th. Stöhlker, H. Backe, H.F. Beyer, F. Bosch, A. Bräuning-Demian, S. Hagmann, D.C. Ionescu, K. Jungmann, H.-J. Kluge, C. Kozhuharov, Th. Kühl, D. Liesen, R. Mann, P.H. Mokler, and W. Quint. Status and perspectives of atomic physics research at gsi: The new {GSI} accelerator project. *Nuclear Instruments and Methods in Physics Research Section B: Beam Interactions with Materials and Atoms*, 205(0):156 – 161, 2003. 11th International Conference on the Physics of Highly Charged Ions.
[40] R.D. Thomas, H.T. Schmidt, G. Andler, M. Bjrkhage, M. Blom, L. Brnnholm, E. Bckstrm, H. Danared, S. Das, N. Haag, P. Halldn, F. Hellberg, A.I.S. Holm, H.A.B. Johansson, A. Kllberg, G. Kllersj, M. Larsson, S. Leontein, L. Liljeby, P. Lfgren, B. Malm, S. Mannervik, M. Masuda, D. Misra, A. Orbn, A. Pal, P. Reinhed, K.-G. Rensfelt, S. Rosn, K. Schmidt, F. Seitz, A. Simonsson, J. Weimer, H. Zettergren, and H. Cederquist. The double electrostatic ion ring experiment: A unique cryogenic electrostatic storage ring for merged ion-beams studies. *Review of Scientific Instruments*, 82(6):–, 2011.
[41] M. Grieser, Yu.A. Litvinov, R. Raabe, K. Blaum, Y. Blumenfeld, P.A. Butler, F. Wenander, and Woods *et al.* (123 more). Storage ring at HIE-ISOLDE. *The European Physical Journal Special Topics*, 207(1):1–117, 2012.

[42] F. Weinhold. Calculation of upper and lower bounds to oscillator strengths. *The Journal of Chemical Physics*, 54(5):1874–1881, 1971.
[43] J.S. Sims, S.A. Hagstrom, and J.R. Rumble, Jr. Upper and lower bounds to atomic properties. iii. li oscillator strengths for various 2s-2p transitions. *Phys. Rev. A*, 13:242–250, 1976.
[44] T. Brage and C. Froese Fischer. Systematic calculations of correlation in complex ions. *Phys. Scr.*, T47:18–28, 1993.
[45] M. Tong, P. Jönsson, and C. Froese Fischer. Convergence studies of atomic properties frop variational methods: total energy, ionization energy, sms and hpf parameters for li. *Phys. Scr.*, 48:446–453, 1993.
[46] T. Brage, C. Froese Fischer, and P. Jönsson. Effects of core-valence and core-core correlation on the line strength of the resonance lines in li i and na i. *Phys. Rev. A*, 49:2181–2184, Mar 1994.
[47] C. Froese Fischer. Convergence studies of mchf calculations for be and li-. *J. Phys. B : At. Mol. Phys.*, 26:855–862, 1993.
[48] M. Godefroid, P. Jönsson, and C. Froese Fischer. Atomic structure variational calculations in spectroscopy. *Phys. Scr.*, T78:33–46, 1998.
[49] M. Godefroid, C. Froese Fischer, and P. Jönsson. Non-relativistic variational calculations of atomic properties in li-like ions: Li i to o vi. *J. Phys. B : At. Mol. Phys.*, 34:1079–1104, 2001.
[50] C. Froese Fischer, S. Verdebout, M. Godefroid, P. Rynkun, P. Jönsson, and G. Gaigalas. Doublet-quartet energy separation in boron: A partitioned-correlation-function-interaction method. *Phys. Rev. A*, 88:062506, Dec 2013.
[51] T. Kato. On the eigenfunctions of many-particle systems in quantum mechanics. *Communications on Pure and Applied Mathematics*, 10(2):151–177, 1957.
[52] C. Froese Fischer. *The Hartree-Fock Method for Atoms. A numerical approach.* John Wiley and Sons, New York, 1977.
[53] P. Jönsson, L. Radžiūtė, G. Gaigalas, M.R. Godefroid, J.P. Marques, T. Brage, C. Froese Fischer, and I.P. Grant. Accurate multiconfiguration calculations of energy levels, lifetimes, and transition rates for the silicon isoelectronic sequence. *A&A*, 585:A26, 2016.
[54] C. Froese Fischer, G. Tachiev, G. Gaigalas, and M.R. Godefroid. An mchf atomic-structure package for large-scale calculations. *Comput. Phys. Commun.*, 176:559–579, 2007.
[55] P. Jönsson, G. Gaigalas, J. Bieroń, C. Froese Fischer, and I.P. Grant. New version: Grasp2K relativistic atomic structure package. *Comput. Phys. Commun.*, 184:2197, 2013.
[56] C. Froese Fischer. B-splines in variational atomic structure calculations. volume 55 of *Advances In Atomic, Molecular, and Optical Physics*, pages 235 – 291. Academic Press, 2008.
[57] B.H. Bransden and C.J. Joachain. *Physics of Atoms and Molecules.* Prentice Hall, Edinburgh Gate, Harlow, England, 2003. second edition.
[58] P.G. Burke and M.J. Seaton. Numerical solutions of the integro-differential equations of electronatom collision theory. *Methods in Computational Physics*, 10:1, 1971.
[59] C. Froese Fischer and M. Idrees. Spline algorithm for continuum function. *Computers in Physics*, 3:53–58, 1989.
[60] G. Breit. The effect of retardation on the interaction of two electrons. *Phys. Rev.*, 34:553–573, Aug 1929.
[61] J.D. Jackson. *Classical Electrodynamics.* John Wiley & Sons, New York, US, 1975. second edition.
[62] I.P. Grant. *Relativistic Quantum Theory of Atoms and Molecules. Theory and Computation.* Atomic, Optical and Plasma Physics. Springer, New York, USA, 2007.
[63] W.R Johnson and G. Soff. The lamb shift in hydrogen-like atoms. *At. Data Nucl. Data Tables*, 33:405–446, 1985.
[64] W.R. Johnson. *Atomic Structure Theory: Lectures on Atomic Physics.* Springer Verlag, Berlin, Heidelberg, Springer-Verlag edition, 2007.
[65] W. Greiner. *Relativistic Quantum Mechanics: Wave Equations.* Springer, 3rd edition, 2000.
[66] R.N. Hill. Hydrogenic wave functions. In G.W.F. Drake, editor, *Atomic, Molecular and Optical Physics Handbook*, pages 153–171. Springer, Berlin, 2006.
[67] H.A. Bethe and E.E. Salpeter. *Quantum Mechanics of One- and Two-electron Atoms.* Springer Verlag, Berlin and New York, 1957.
[68] B.J. McKenzie, I.P. Grant, and P.H. Norrington. A program to calculate transverse Breit and QED corrections to energy levels in a multiconfiguration Dirac-Fock environment. *Computer Physics Communications*, 21(2):233–246, 12 1980.
[69] Peter J. Mohr. Self-energy of the $n = 2$ states in a strong coulomb field. *Phys. Rev. A*, 26:2338–2354, Nov 1982.

[70] Peter J. Mohr and Yong-Ki Kim. Self-energy of excited states in a strong coulomb field. *Phys. Rev. A*, 45:2727–2735, Mar 1992.
[71] Éric-Olivier Le Bigot, Paul Indelicato, and Peter J. Mohr. Qed self-energy contribution to highly excited atomic states. *Phys. Rev. A*, 64:052508, Oct 2001.
[72] J.A. Lowe, C.T. Chantler, and I.P. Grant. Self-energy screening approximations in multi-electron atoms. *Radiation Physics and Chemistry*, 85(0):118 – 123, 2013.
[73] V. M. Shabaev, I. I. Tupitsyn, and V. A. Yerokhin. Model operator approach to the lamb shift calculations in relativistic many-electron atoms. *Phys. Rev. A*, 88:012513, Jul 2013.
[74] V.M. Shabaev, I.I. Tupitsyn, and V.A. Yerokhin. Qedmod: Fortran program for calculating the model lamb-shift operator. *Computer Physics Communications*, 189:175 – 181, 2015.
[75] E. A. Uehling. Polarization effects in the positron theory. *Phys. Rev.*, 48:55–63, Jul 1935.
[76] L. Wayne Fullerton and G. A. Rinker. Accurate and efficient methods for the evaluation of vacuum-polarization potentials of order $z\alpha$ and $z\alpha^2$. *Phys. Rev. A*, 13:1283–1287, Mar 1976.
[77] P. Jönsson, X. He, C. Froese Fischer, and I.P. Grant. The grasp2k relativistic atomic structure package. *Comput. Phys. Commun.*, 177:597–622, 2007.
[78] A.I. Akhiezer and V.B. Berestetskii. *Quantum Electrodynamics*. Interscience, New York, 1965.
[79] L. Armstrong Jr. and S. Feneuille. Relativistic effects in the many-electron atom. *Adv. At. Mol. Phys.*, 10:1, 1974.
[80] R. Glass and A. Hibbert. Relativistic effects in many electron atoms. *Comput. Phys. Commun.*, 16:19–34, 1978.
[81] R.R. Moss. *Advanced Molecular Quantum Mechanics. An Introduction on Relativistic Quantum Mechanics and the Quantum Theory of Radiation*. Chapman and Hall, London, 1973.
[82] A. Hibbert. *Isoelectronic Trends in Atomic Properties*. Taylor & Francis, 2016/01/19 2011.
[83] W. Pauli. ber den zusammenhang des abschlusses der elektronengruppen im atom mit der komplexstruktur der spektren. *Zeitschrift fr Physik*, 31(1):765–783, 1925.
[84] C. Froese Fischer, T. Brage, and P. Jönsson. *Computational Atomic Structure: An MCHF Approach*. Institute of Physics Publishing, Bristol and Philadelphia, 1997.
[85] G. Gaigalas and C. Froese Fischer. Extension of the {HF} program to partially filled f-subshells. *Computer Physics Communications*, 98(12):255 – 264, 1996.
[86] G. Racah. Theory of complex spectra. iii. *Phys. Rev.*, 63:367–382, May 1943.
[87] R. D. Cowan. *The Theory of Atomic Structure and Spectra*. Los Alamos Series in Basic and Applied Sciences. University of California Press, 1981.
[88] A.P. Jucys, I. Levinson, and V. Vanagas. *Mathematical Apparatus of the Angular Momentum Theory*. Israel Program for Scientific Translations, Jerusalem, 1963.
[89] G. Racah. Theory of complex spectra. iv. *Phys. Rev.*, 76:1352–1365, Nov 1949.
[90] B.R. Judd. *Operator Techniques in Atomic Spectroscopy*. Princeton Landmarks in Physics. Princeton University Press, Princeton, New Jersey, 1998.
[91] B.R. Judd. *Second Quantization and Atomic Spectroscopy*. The Johns Hopkins Press, Baltimore, MD, 1967.
[92] B.R. Judd. Complex atomic spectra. *Reports on Progress in Physics*, 48(7):907, 1985.
[93] B.R. Judd. Lie groups for atomic shells. *Physics Reports*, 285(12):1 – 76, 1997.
[94] Z.B. Rudzikas. *Theoretical Atomic Spectroscopy*. Cambridge Monographs on Atomic, Molecular and Chemical Physics. Cambridge University Press, Cambridge, 1997.
[95] G. Gaigalas and Z. Rudzikas. On the secondly quantized theory of the many-electron atom. *J. Phys. B : At. Mol. Phys.*, 29:3303–3318, 1996.
[96] U. Fano. Interaction between configurations with several open shells. *Phys. Rev. A*, 140:67–75, 1965.
[97] J.J. Sakurai. *Modern Quantum Mechanics*. The Benjamin-Cummings Publishing Company, Inc., Menlo Park, 1985.
[98] R.K. Nesbet. *Variational Principles and Methods in Theoretical Physics and Chemistry*. Cambridge University Press, Cambridge, UK, 2004.
[99] D.R. Hartree. *The calculation of atomic structures*. John Wiley and Sons, New York, 1957.
[100] J.C. Slater. *Quantum Theory of Atomic Structure - Vol.I*. McGraw–Hill, New York, 1960.
[101] G. Gaigalas, Z. Rudzikas, and C. Froese Fischer. An efficient approach for spin-angular integrations in atomic structure calculations. *J. Phys. B : At. Mol. Phys.*, 30:3747–71, 1997.
[102] C. Froese Fischer. A B-spline Hartree-Fock program. *Comput. Phys. Commun.*, 182:1315–1326, 2011.
[103] T. Koopmans. ber die zuordnung von wellenfunktionen und eigenwerten zu den einzelnen elektronen eines atoms. *Physica*, 1(16):104 – 113, 1934.

[104] J.C. Phillips. Generalized koopmans' theorem. *Phys. Rev.*, 123:420–424, Jul 1961.
[105] C. Froese Fischer. Self-consistent-field (SCF) and multiconfiguration (MC) Hartree-Fock (HF) methods in atomic calculations: Numerical integration approaches. *Comp. Phys. Rep.*, 3(5):274, 6 1986.
[106] J. Bauche and M. Klapisch. Remarks on brillouin's theorem in the atomic variational approach. *J. Phys. B : At. Mol. Phys.*, 5:29–36, 1972.
[107] J.J. Labarthe. Brillouin's theorem for inter-shell correlations in the hartree-fock method. *J. Phys. B : At. Mol. Phys.*, 5:L181–2, 1972.
[108] C. Froese Fischer. Brillouin's theorem for excited (nl) q (n'l) q ' configurations. *Journal of Physics B: Atomic and Molecular Physics*, 6(10):1933, 1973.
[109] M. Godefroid, J. Liévin, and J.-Y. Metz. Brillouin's theorem for complex atomic configurations. *J. Phys. B : At. Mol. Phys.*, 20:3283–3296, 1987.
[110] J.M. Kaniauskas, V.C. Simonis, and Z.B. Rudzikas. Isospin method for complex electronic configurations. *J. Phys. B : At. Mol. Phys.*, 20:3267, 1987.
[111] G. Gaigalas, S. Fritzsche, E. Gaidamauskas, G. Kiršanskas, and T. Žalandauskas. Jahn - a program for representing atomic and nuclear states within an isospin basis. *Computer Physics Communications*, 175(1):52 – 66, 2006.
[112] G. Gaigalas, S. Fritzsche, and Z. Rudzikas. Reduced coefficients of fractional parentage and matrix elements of the tensor w(kqkj) in jj-coupling. *Atomic Data and Nuclear Data Tables*, 76(2):235 – 269, 2000.
[113] G. Gaigalas, S. Fritzsche, and I. P. Grant. Program to calculate pure angular momentum coefficients in jj-coupling. *Comput. Phys. Commun.*, 139:263–278, 2001.
[114] E.A. Hylleraas and B. Undheim. Numerische berechnung der 2s-terme von ortho- und parhelium. *Zeitschrift für Physik*, 65(11-12):759–772, 1930.
[115] J. K. L. MacDonald. Successive approximations by the rayleigh-ritz variation method. *Phys. Rev.*, 43:830–833, May 1933.
[116] A.S. Coolidge and H.M. James. Wave functions for $1s2s\ ^1s$ helium. *Phys. Rev.*, 49:676–687, May 1936.
[117] C. Froese Fischer. Mchf correlation study of 1s2s 1s. *Can. J. Phys.*, 51:1238–1243, 1973.
[118] C. Froese Fischer. Perturbers in (2d)nd 3p rydberg series of s. *J. Phys. B : At. Mol. Phys.*, 20:4365–4374, 1987.
[119] C. Froese Fischer. Oscillator-strength trends in the presence of level crossings. *Phys. Rev. A*, 22:551–556, Aug 1980.
[120] R.D. Cowan and J.E. Hansen. Discrete-continuum interactions in Cl I and S I. *J. Opt. Soc. Am. B*, 71:60, 1981.
[121] B.O. Roos, P.R. Taylor, and P.E.M. Siegbahn. A complete active space {SCF} method (casscf) using a density matrix formulated super-ci approach. *Chemical Physics*, 48(2):157 – 173, 1980.
[122] C. Froese Fischer. The solution of Schrodinger's equation for two–electron systems by an MCHF procedure. *JCoP*, 13:502–521, 1973.
[123] P.O. Löwdin. Quantum Theory of Many-Particle Systems. I. Physical Interpretations by Means of Density Matrices, ... *Phys. Rev.*, 97:1474–89, 1955.
[124] A. Borgoo, O. Scharf, G. Gaigalas, and M. Godefroid. Multiconfiguration electron density function for the ATSP2K-package. *Comput. Phys. Commun.*, 181:426–439, 2010.
[125] A. Hibbert, C. Froese Fischer, and M. Godefroid. Non-orthogonal orbitals in mchf or configuration interaction wave functions. *Comput. Phys. Commun.*, 51:285–293, 1988.
[126] J. Olsen, B.O. Roos, P. Jørgensen, and H.J.Aa. Jensen. Determinant based ci algorithms for cas and ras spaces. *J. Chem. Phys.*, 89:2185–92, 1988.
[127] N. Vaeck, M. Godefroid, and J.E. Hansen. Multiconfiguration hartree-fock calculations for singlet terms in neutral strontium. *Phys. Rev. A*, 38:2830–2845, Sep 1988.
[128] N. Vaeck, M. Godefroid, and C. Froese Fischer. Core-valence correlation effects on e1 and e2 decay rates in ca^+. *Phys. Rev. A*, 46:3704–16, 1992.
[129] A. Stathopoulos and C. Froese Fischer. A davidson program for finding a few selected extreme eigenpairs of a large, sparse, real, symmetric matrix. *Computer Physics Communications*, 79(2):268 – 290, 1994.
[130] A. Stathopoulos, Y. Saad, and C. Froese Fischer. Robust preconditioning of large, sparse, symmetric eigenvalue problems. *Journal of Computational and Applied Mathematics*, 64(3):197 – 215, 1995.
[131] C. Froese Fischer and G. Tachiev. Breit-pauli energy levels, lifetimes, and transition probabilities for the beryllium-like to neon-like sequences. *At. Data Nucl. Data Tables*, 87:1–184, 2004.

[132] M Godefroid. Note on the mutual spin-orbit matrix elements. *Journal of Physics B: Atomic and Molecular Physics*, 15(20):3583, 1982.

[133] A. Hibbert, R. Glass, and C. Froese Fischer. A general program for computing angular integrals of the Breit-Pauli Hamiltonian. *Comput. Phys. Commun.*, 64:455–472, 1991.

[134] G. Gaigalas, Z. Rudzikas, and C. Froese Fischer. Reduced coefficients (subcoefficients) of fractional parentage for p-, d-, and f-shells. *At. Data Nucl. Data Tables*, 70:1–39, 1998.

[135] O. Zatsarinny and C. Froese Fischer. A general program for computing angular integrals of the BreitPauli Hamiltonian with non-orthogonal orbitals. *Comput. Phys. Commun.*, 124:247–289, 2000.

[136] C. Froese Fischer, G. Tachiev, and A. Irimia. Relativistic energy levels, lifetimes and transition probabilities for the sodium-like to argon-like sequences. *At. Data Nucl. Data Tables*, 92:607, 2006.

[137] P. Indelicato and J.P. Desclaux. Projection operator in the multiconfiguration dirac-fock method. *Physica Scripta*, 1993(T46):110, 1993.

[138] P. Indelicato. Projection operators in multiconfiguration Dirac-Fock calculations: Application to the ground state of heliumlike ions. *Phys. Rev. A*, 51(2):1132–1145, 1995.

[139] F.A. Parpia, C. Froese Fischer, and I.P. Grant. GRASP92: A package for large-scale relativistic atomic structure calculations. *Comput. Phys. Commun.*, 94:249–271, 1996.

[140] A. Ynnerman and C. Froese Fischer. Multiconfigurational-dirac-fock calculation of the $2s^2\ ^1s_0\breve{}2\ s\ 2\ p\ ^3p_1$ spin-forbidden transition for the be-like isoelectronic sequence. *Phys. Rev. A*, 51:2020–2030, Mar 1995.

[141] C. Froese Fischer. Relativistic calculations for highly charged ions. *Nuclear Instruments and Methods in Physics Research B*, 235:100–104, JUL 2005. 12th International Conference on the Physics of Highly Charged Ions, Vilnius, LITHUANIA, SEP 06-11, 2004.

[142] C. Froese Fischer, G. Gaigalas, and Y. Ralchenko. Some corrections to grasp92. *Comput. Phys. Commun.*, 175(11-12):738–744, DEC 2006.

[143] Y.-K. Kim, D.H. Baik, P. Indelicato, and J.P. Desclaux. Resonance transition energies of li-, na-, and cu-like ions. *Phys. Rev. A*, 44:148–166, Jul 1991.

[144] P. Indelicato, J. P. Santos, S. Boucard, and J.-P. Desclaux. Qed and relativistic corrections in superheavy elements. *The European Physical Journal D*, 45(1):155–170, 2007.

[145] I.P. Grant. Relativistic calculation of atomic properties. *Computer Physics Communications*, 84:59 – 77, 1994.

[146] T. Carette, M. Nemouchi, J. Li, and M. Godefroid. Relativistic effects on the hyperfine structures of $2p^4\ ^3p)3p,^2\ D^o,^4\ D^o$, and $^4P^o$ in ^{19}f i. *Phys. Rev. A*, 88:042501, Oct 2013.

[147] I.P. Grant, B.J. Mc Kenzie, P.H. Norrington, D.F. Mayers, and N.C. Pyper. An atomic multiconfigurational dirac-fock package. *Comput. Phys. Commun.*, 21:207, 1980.

[148] Ekman, J., Jönsson, P., , Gustafsson, S., Hartman, H., Gaigalas, G., and Godefroid, M. R. Froese Fischer, C. Calculations with spectroscopic accuracy: energies, transition rates, and landé g_j-factors in the carbon isoelectronic sequence from ar xiii to zn xxv. *A&A*, 564:A24, 2014.

[149] L. Radžiūtė, J. Ekman, P. Jönsson, and G. Gaigalas. Extended calculations of level and transition properties in the nitrogen isoelectronic sequence: Cr XVIII, Fe XX, Ni XXII, and Zn XXIV. *A&A*, 582:A61, 2015.

[150] G. Gaigalas, T. Žalandauskas, and Z. Rudzikas. Ls - jj transformation matrices for a shell of equivalent electrons. *Atomic Data and Nuclear Data Tables*, 84(2):99 – 190, 2003.

[151] P.O. Löwdin. Quantum Theory of Many-Particle Systems. III. Extension of the HF Scheme to Include Degenerate Systems and Correlation Effects. *Phys. Rev.*, 97:1509–1520, 1955.

[152] O. Sinanoglu and I. Oksuz. Theory of atomic structure including electron correlation. *Phys. Rev. Lett.*, 21:507–511, 1968.

[153] C.A. Nicolaides. State- and Property-Specific Quantum Chemistry. In J.R. Sabin and E. Brändas, editors, *Advances in Quantum Chemistry*, volume 62, chapter 2, pages 35–103. Academic Press, San Diego, 2011.

[154] C. Schwartz. Estimating convergence rates of variational calculations. In S. Fernbach B. Alder and M. Rotenburg, editors, *Methods in Computational Chemistry - vol. 2*, page 241. Academic Press, New York, 1963.

[155] A. Messiah. *Quantum Mechanics*. Dover Publications, Inc., Mineola, New York, 2014.

[156] D. Layzer, Z. Horak, M.N. Lewis, and D.P. Thompson. Second-Order Z-Dependent Theory of Many-Electron Atoms. *Adv. Phys.*, 29:101, 1964.

[157] L. Sturesson and C. Froese Fischer. LSGEN: A program to generate configuration state lists of LS coupled basis functions. *Comput. Phys. Commun.*, 74:432, 1993.

[158] L. Sturesson, P. Jönsson, and C. Froese Fischer. Jjgen: A flexible program for generating lists

of jj-coupled configuration state functions. *Computer Physics Communications*, 177(6):539 – 550, 2007.

[159] S. Verdebout, P. Jönsson, G. Gaigalas, M. Godefroid, and C. Froese Fischer. Exploring biorthonormal transformations of pair-correlation functions in atomic structure variational calculations. *J. Phys. B : At. Mol. Phys.*, 43:074017, 2010.

[160] S. Verdebout, P. Rynkun, P. Jönsson, G. Gaigalas, C. Froese Fischer, and M. Godefroid. A partitioned correlation function interaction approach for describing electron correlation in atoms. *Journal of Physics B: Atomic, Molecular and Optical Physics*, 46(8):085003, 2013.

[161] J. Olsen, M. Godefroid, P. Jönsson, P.-Å. Malmqvist, and C. Froese Fischer. Transition probability calculations for atoms using non-orthogonal orbitals. *Phys. Rev. E*, 52:4499–4508, 1995.

[162] T. Brage, C. Froese Fischer, N. Vaeck, M. Godefroid, and A. Hibbert. Core polarization in ca i and ca ii. *Phys. Scr.*, 48:533–545, 1993.

[163] M. Godefroid, J. Olsen, P. Jönsson, and C. Froese Fischer. Accurate mchf gf-values ... b ii line at 1362 a. *Astrophys. J*, 450:473–6, 1995.

[164] M. Godefroid, G. Van Meulebeke, P. Jönsson, and C. Froese Fischer. Large-scale mchf calculations of hyperfine structures in nitrogen and oxygen. *Z. Phys.D–Atoms, Molecules and Clusters*, 42:193–201, 1997.

[165] T. Carette and M. Godefroid. Theoretical study of the C^- $^4S_{3/2}$ and $^2D_{3/2,5/2}$ bound states and C ground configuration: Fine and hyperfine structures, isotope shifts, and transition probabilities. *Physical Review A*, 83:062505, 2011.

[166] T Carette and M R Godefroid. Isotope shift on the chlorine electron affinity revisited by an mchf/ci approach. *Journal of Physics B: Atomic, Molecular and Optical Physics*, 46(9):095003, 2013.

[167] S.R. Langhoff and E.R. Davidson. Configuration interaction calculations on the nitrogen molecule. *International Journal of Quantum Chemistry*, 8(1):61–72, 1974.

[168] L. Meissner. Size-consistency corrections for configuration interaction calculations. *Chemical Physics Letters*, 146(34):204 – 210, 1988.

[169] L. Radžiūtė, D. Kato, G. Gaigalas, P. Jönsson, P. Rynkun, V. Jonauskas, and S. Kučas. Energy level structure of the ground configuration in the er 3+ free ion. *Physica Scripta*, 90(5):054001, 2015.

[170] Yu Zou and C. Froese Fischer. Resonance transition energies and oscillator strengths in lutetium and lawrencium. *Phys. Rev. Lett.*, 88:183001, Apr 2002.

[171] M. S. Safronova, U. I. Safronova, and Charles W. Clark. Correlation effects in la, ce, and lanthanide ions. *Phys. Rev. A*, 91:022504, Feb 2015.

[172] P. Jönsson, J. Ekman, S. Gustafsson, H Hartman, L.B. Karlsson, R. du Rietz, G. Gaigalas, M.R. Godefroid, and C. Froese Fischer. Energy levels and transition rates for the boron isoelectronic sequence: Si x, ti xviii - cu xxv. *A&A*, 559:A100, 2013.

[173] P. Jönsson, P. Bengtsson, J. Ekman, S. Gustafsson, L.B. Karlsson, G. Gaigalas, C. Froese Fischer, D. Kato, I. Murakami, H.A. Sakaue, H. Hara, T. Watanabe, N. Nakamura, and N. Yamamoto. Relativistic {CI} calculations of spectroscopic data for the and configurations in ne-like ions between mg {III} and kr {XXVII}. *Atomic Data and Nuclear Data Tables*, 100(1):1 – 154, 2014.

[174] M. Godefroid and C. Froese Fischer. Isotope shift in the oxygen electron affinity. *Phys. Rev. A*, 60:R2637–2640, 1999.

[175] C. Blondel, C. Delsart, C. Valli, S. Yiou, M.R. Godefroid, and S. Van Eck. Electron affinities of $^{16,17,18}O$, the fine structure of $^{16}O^-$ and the hyperfine structure of $^{17}O^-$. *Phys. Rev. A*, 64:052504/1–14, 2001.

[176] J. Li, C. Nazé, M. Godefroid, S. Fritzsche, G. Gaigalas, P. Indelicato, and P. Jönsson. Mass- and field-shift isotope parameters for the $2s-2p$ resonance doublet of lithiumlike ions. *Phys. Rev. A*, 86:022518, Aug 2012.

[177] C. Nazé, S. Verdebout, P. Rynkun, G. Gaigalas, M. Godefroid, and P. Jönsson. Isotope shifts in beryllium-, boron-, carbon-, and nitrogen-like ions from relativistic configuration interaction calculations. *Atomic Data and Nuclear Data Tables*, 100(5):1197 – 1249, 2014.

[178] C. Nazé, J. G. Li, and M. Godefroid. Theoretical isotope shifts in neutral barium. *Phys. Rev. A*, 91:032511, Mar 2015.

[179] T. Carette, M. Nemouchi, P. Jönsson, and M. Godefroid. Saturation spectra of low lying states of nitrogen: reconciling experiment with theory. *Eur. Phys. J. D*, 60:231–242, 2010.

[180] S. Verdebout, C. Nazé, P. Jönsson, P. Rynkun, M. Godefroid, and G. Gaigalas. Hyperfine structures and landé -factors for states in beryllium-, boron-, carbon-, and nitrogen-like ions from relativistic configuration interaction calculations. *Atomic Data and Nuclear Data*

Compiled on 2016/01/23 at 13:08:13

Tables, 100(5):1111 – 1155, 2014.

[181] J. Bieroń, C. Froese Fischer, S. Fritzsche, G. Gaigalas, I.P. Grant, P. Indelicato, P. Jönsson, and P. Pyykkö. Ab initio mcdhf calculations of electronnucleus interactions. *Physica Scripta*, 90(5):054011, 2015.

[182] M. Andersson, J. Grumer, N. Ryde, R. Blackwell-Whitehead, R. Hutton, Y. Zou, P. Jönsson, and T. Brage. Hyperfine-dependent gf-values of mn i lines in the 1.49-1.80 μm h band. *The Astrophysical Journal Supplement Series*, 216(1):2, 2015.

[183] J. Li, C. Dong, P. Jönsson, and G. Gaigalas. M_F-dependent hyperfine induced transition rates in an external magnetic field for Be-like Titane. *Physics Letters A*, 375(5):914 – 917, 2011.

[184] J. Grumer, W. Li, D. Bernhardt, J. Li, S. Schippers, T. Brage, P. Jönsson, R. Hutton, and Y. Zou. Effect of an external magnetic field on the determination of e1m1 two-photon decay rates in be-like ions. *Phys. Rev. A*, 88:022513, Aug 2013.

[185] O. Zatsarinny and C. Froese Fischer. Atomic structure calculations using {MCHF} and {BSR}. *Computer Physics Communications*, 180(11):2041 – 2065, 2009.

[186] O. Zatsarinny and K. Bartschat. The b -spline r -matrix method for atomic processes: application to atomic structure, electron collisions and photoionization. *Journal of Physics B: Atomic, Molecular and Optical Physics*, 46(11):112001, 2013.

[187] K. Zatsarinny, O.and Bartschat. Relativistic b-spline r-matrix method for electron collisions with atoms and ions: Application to low-energy electron scattering from cs. *Phys. Rev. A*, 77:062701, Jun 2008.

[188] O. Zatsarinny and C. Froese Fischer. DBSR_HF: A B-spline Dirac-Hartree-Fock program. *Computer Physics Communications*, 2016. submitted.